

The Laurentide Ice Sheet in southern New England and New York during and at the end of the Last Glacial Maximum - A cosmogenic-nuclide chronology

Allie Balter-Kennedy^{1,2}, Joerg M. Schaefer^{1,2}, Greg Balco³, Meredith A. Kelly⁴, Michael R. Kaplan¹, Roseanne Schwartz¹, Bryan Oakley⁵, Nicolás E. Young¹, Jean Hanley¹, Arianna M. Varuolo-Clarke^{1,2}

¹Lamont–Doherty Earth Observatory, Columbia University, Palisades, NY 10964, USA

²Department of Earth and Environmental Sciences, Columbia University, New York, NY 10027, USA

³Berkeley Geochronology Center, Berkeley, CA 94709 USA.

⁴Department of Earth Sciences, Dartmouth College, Hanover, NH 03755, USA

⁵Environmental Earth Science Department, Eastern Connecticut State University, Willimantic, CT, 06226, USA

Correspondence to: Allie Balter-Kennedy (abalter@ldeo.columbia.edu)

Abstract. We present 40 new ¹⁰Be exposure ages of moraines and other glacial deposits left behind by the southeastern sector of the Laurentide Ice Sheet (LIS) in southern New England and New York, summarize the regional moraine record, and interpret the dataset in the context of previously published deglaciation chronologies. The regional moraine record spans the Last Glacial Maximum (LGM), with the outermost ridge of the terminal complex dating to ~26–25 ka, the innermost ridge of the terminal complex dating to ~22 ka, and a series of smaller recessional limits within ~50 km of the terminal complex dating to ~21–20.5 ka. The chronology generally agrees with independent age constraints from radiocarbon and glacial varves. A few inconsistencies among ages from cosmogenic-nuclide measurements and those from other dating methods are explained by geologic scatter where several bedrock samples and boulders from the outer terminal moraine exhibit nuclide inheritance, while some exposure ages on large moraines are likely affected by postdepositional disturbance. The exposure-age chronology places the southeastern sector of the LIS at or near its maximum extent from ~26 to 21 ka, which is broadly consistent with the LGM sea-level lowstand, local and regional temperature indicators, and local summer insolation. The net change in LIS extent represented by this chronology occurred more slowly (<5 to 25 m yr⁻¹) than subsequent retreat through the rest of New England, consistent with a slow general rise in insolation and modeled summer temperature. We conclude that the major pulse of LIS deglaciation and accelerated recession, recorded by dated glacial deposits north of the moraines discussed here, did not begin until after atmospheric CO₂ increased at ~18 ka, marking the onset of Termination 1.

Short Summary. We date sedimentary deposits indicating the southeastern Laurentide Ice Sheet was at or near its southernmost extent from ~26,000 to 21,000 years ago when sea-level was lowest and other climate records indicate glacial conditions. Slow deglaciation began ~22,000 years ago alongside a slow but steady rise in modeled local

35 summer temperature, but significant deglaciation in the region did not begin until ~18,000 years ago when atmospheric
36 CO₂ began to rise, signaling the end of the last ice age.

37 **1 Introduction**

38 We describe new cosmogenic-nuclide exposure ages on moraines and other glacial-margin deposits in
39 southern New England and New York that track the timing and position of the margin of the southeastern sector of
40 the Laurentide Ice Sheet (LIS) during the Last Glacial Maximum (LGM; 26.5–19 ka) and Termination 1 (18–11 ka),
41 the most recent glacial-interglacial transition. The LIS held ~50–80 m sea-level equivalent at its greatest extent during
42 the LGM (Clark et al., 2009, 1996; Denton and Hughes, 1981; Stokes, 2017; Stokes et al., 2012), making it the largest
43 ice sheet of the last glacial period, and then deglaciated as temperature and CO₂ returned to interglacial values during
44 Termination 1 (Broecker and Donk, 1970; Cuffey et al., 2016; Dalton et al., 2020; Denton et al., 2010; Dyke, 2004;
45 Marcott et al., 2014). LIS topography, albedo, and meltwater exerted major forcing on large-scale atmospheric
46 dynamics (Löfverström et al., 2014; Ullman et al., 2014), ocean circulation (Clark et al., 2001; Denton et al., 2010;
47 McManus et al., 2004), and sea-level (Clark et al., 2009; Lambeck et al., 2014; Stokes, 2017) during the LGM and
48 subsequent deglaciation. We focus on the southeastern sector of the LIS, which is important in part because of its
49 proximity to the North Atlantic Ocean, meaning that meltwater from this sector had the potential to suppress the
50 Atlantic Meridional Overturning Circulation (AMOC), inducing global-scale climate feedbacks (Barker et al., 2009;
51 Barker and Knorr, 2021; Buizert et al., 2014; Denton et al., 2010; McManus et al., 2004). Improving LIS chronologies
52 thus bears on better understanding of regional and hemispheric paleoenvironmental and paleoclimatic changes.

53 Cosmogenic-nuclide and radiocarbon dating have been used to show that the LIS fluctuated at or near its full
54 LGM extent until ~22 ka, with terminal moraines dating to ~23–22 ka in the midwestern United States (Curry and
55 Petras, 2011; Glover et al., 2011; Heath et al., 2018; Ullman et al., 2015) and to ~26–24 ka in the northeastern United
56 States (Balco et al., 2002; Balco and Schaefer, 2006; Corbett et al., 2017; Stanford et al., 2021). Margin retreat
57 potentially accelerated across the LIS by ~20.5 ka (Balco and Schaefer, 2006; Ullman et al., 2015). Therefore, the
58 initial retreat of the LIS margin from its LGM limits coincided with a steady rise in boreal summer insolation that
59 began ~24 ka (Clark et al., 2009; Denton et al., 2010; Hays et al., 1976; Milankovitch, 1941; Ullman et al., 2015), and
60 began several thousand years before the deglacial rise in CO₂ observed in the Antarctic ice core record (Marcott et al.,
61 2014). The LIS might have been sensitive to this relatively weak orbital forcing in its full glacial configuration,
62 although orbital forcing alone was likely insufficient to force the return to full interglacial conditions (Barker and
63 Knorr, 2021; Denton et al., 2010; Imbrie et al., 1993; Raymo, 1997; Tzedakis et al., 2018). The increase in atmospheric
64 CO₂ beginning around 18 ka likely played a key role in the full deglaciation of the LIS (Gregoire et al., 2015; Marcott
65 et al., 2014; Shakun et al., 2015).

66 Prominent moraines in northern New Jersey, and coastal New York and New England, along with a series of
67 smaller recessional moraines, mark the LIS extent during the LGM and afford an opportunity to constrain the timing
68 of the LGM and initial deglaciation during Termination 1. These moraines are morphostratigraphically correlated across
69 the region and bracketing radiocarbon ages from a few locations have been used to estimate the ages for the entire
70 moraine sequence (Stone and Borns, 1986; Stone et al., 2005). Several of the moraine segments have now also been

71 dated using cosmogenic nuclides (Balco et al., 2009, 2002; Balco and Schaefer, 2006; Corbett et al., 2017). Our 40
72 new ¹⁰Be ages from Rhode Island, Long Island, New York City, and the Lower Hudson Valley complement existing
73 moraine chronologies for the LIS margin and, together, these chronologies provide net changes in LIS extent as well
74 as retreat rate estimates for this climatically important sector.

75 **1.1 Existing LIS chronologies in southern New England, New York, and northern New Jersey**

76 **1.1.1 Regional moraine stratigraphy**

77 Regional LIS margin positions have been inferred across the northeastern United States using various glacial
78 deposits, including moraines, glacial lake sediment, ice-contact deltas, and morphosequences of contemporaneous ice-
79 marginal to -distal landforms and sediment facies (e.g., Cadwell, 1989; Fuller, 1914; Koteff and Pessl, 1981;
80 McMaster, 1960; Stone and Borns, 1986; Stone et al., 2005; Woodworth and Wigglesworth, 1934). Importantly, these
81 deposits mark the most recent extension of the ice margin to a given position because each advance of the ice sheet
82 removes evidence of previous ice-margin fluctuations. The most prominent of these features is a terminal moraine
83 complex that defines the modern coastline of New England and New York, composed of two massive end moraine
84 systems that were constructed during the most extensive LGM advances of the Hudson, Connecticut, and
85 Narragansett-Buzzards Bay lobes. These large moraines (50–100 m tall, 2–10 km wide) are characterized by
86 imbricated thrust sheets of outwash deposits and dislocated preglacial sediment displaced during ice-margin advance
87 and are overlain by till in many places (Fuller, 1914; Kaye, 1972, 1964a, 1964b; Mills and Wells, 1974; Oldale and
88 O’Hara, 1984; Sirkin, 1982; Boothroyd and Sirkin, 2002). Crosscutting relationships among segments within the
89 moraine systems and, importantly, the glaciotectionic nature of the deposits combined with the presence of overlying
90 till suggest that the moraines were formed during phases of ice-margin advance as the LIS fluctuated at or near its
91 southernmost reaches during the last glaciation (Oldale and O’Hara, 1984; Sirkin, 1976; Boothroyd and Sirkin, 2002).
92 The outermost component of the terminal complex can be traced from the Budd Lake moraine in northern New Jersey,
93 to the Harbor Hill and Ronkonkoma moraines on Long Island, New York and across Block Island Sound to Martha’s
94 Vineyard and Nantucket (Figure 1; Stone and Borns, 1986). About 10–30 km north of the outer terminal limit, the
95 innermost element of the terminal moraine complex records the last major LGM ice advance in the region and is
96 correlated across Long Island’s north shore to Fisher’s Island, Connecticut, the Charlestown moraine in Rhode Island,
97 and the Buzzards Bay moraine on Cape Cod (Figure 1; Sirkin, 1976; Sirkin, 1982; Stone and Borns, 1986).

98 A series of ice-contact deltas has been used to correlate the ice-margin position along Long Island’s north
99 shore across New York City to the Ogdensburg-Culvers Gap moraine in northern New Jersey (Figure 1; Stanford,
100 1993; Stanford et al., 2021; Stone et al., 1995, 2005). The easternmost of these deltas in lower Manhattan is associated
101 with glacial Lake Bayonne, the presence of which required that the ice margin was located at or south of the Sands
102 Point moraine on Long Island to block a spillway at Hell Gate (Figure 1; Stanford et al., 2021; Stanford and Harper,
103 1991; Stone et al., 2005). The large coastal moraines dammed lakes fed by LIS meltwater as the ice-margin retreated
104 northward, and the associated lakefloor deposits are found throughout northern New Jersey (Stanford et al., 2021) and
105 underlie much of what is now Long Island Sound (Stone et al., 2005), Narragansett Bay (Oakley, 2012), Block Island
106 Sound, and Rhode Island Sound (Needell et al., 1983; Frankel and Thomas, 1966)

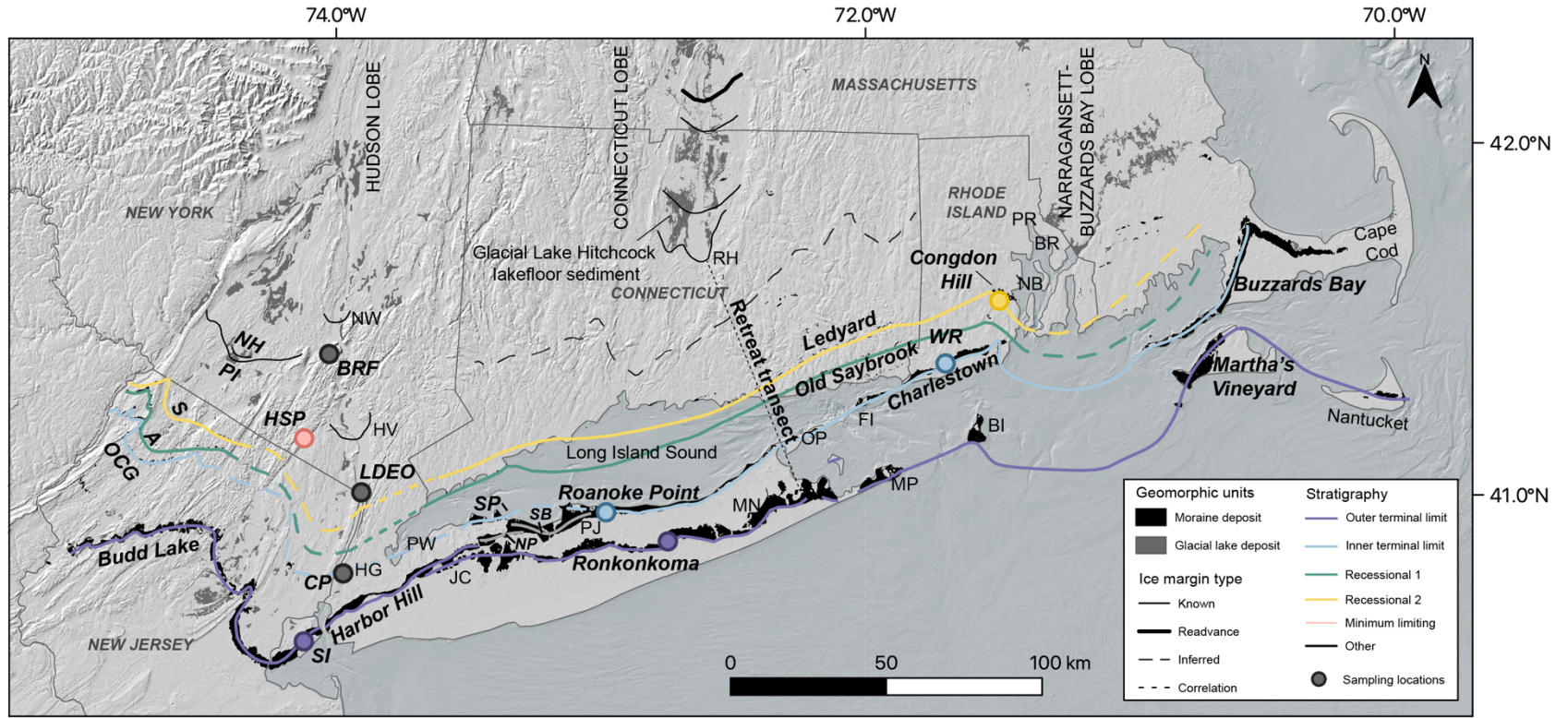


Figure 1 - Regional map of New England and New York depicting ice marginal positions and glacial geomorphology. Hillshade topography from NASA Shuttle Radar Topography Mission (2013). Bathymetry from NOAA Office of Coast Survey BlueTopo product (tinted dark blue to indicate ocean). Glacial geology is from the surficial geologic maps of Massachusetts (Stone et al., 2018), Rhode Island (Boothroyd et al., 2003), Connecticut (Stone et al., 2005), New York (Cadwell et al., 1989), and New Jersey (Stone et al., 2002). Ice marginal positions and correlations are adapted from Sirkin (1982), Stone and Borns (1986), Boothroyd et al. (1998), Stone et al. (2005), Ridge et al. (2004), Ridge et al. (2012), and Stanford et al. (2021). Retreat rates presented in Section 5.1.3 are calculated using distance along the retreat transect. Moraine segment names discussed in the text are labeled in bold italics and other locations of relevance are labeled in regular text. Sample locations associated with a specific ice-margin position discussed in the text are colored by their stratigraphy as defined in the legend. A = Augusta moraine, BI = Block Island, BR = Barrington, RI, BRF = Black Rock Forest, CP = Central Park, FI = Fishers Island, HG = Hell Gate, HSP = Harriman State Park, HV = Haverstraw, NY, JC = Jericho, NY, LDEO = Lamont-Doherty Earth Observatory, MP = Montauk Point, MN = Manorville, NY, NB = Narragansett Bay, NW = Newburgh, NY, NH = New Hampton moraine, NP = Northport moraine, OCG = Ogdensburg-Culvers Gap moraine, OP = Orient Point, PI = Pellets Island moraine, PJ = Port Jefferson, NY, PW = Port Washington, NY, RH = Rocky Hill, CT, S = Sussex moraine, SB = Stony Brook moraine, SI = Staten Island, SP = Sands Point moraine, WR = Wolf Rocks Moraine.

Ice-margin positions north of the terminal complex are marked by smaller moraines and other ice-marginal landforms that are different in character from the large coastal moraines. Several discontinuous (individual segments up to 3 km in length), boulder-rich moraines are interpreted as recording brief readvances or standstills as the Connecticut and Narragansett-Buzzards Bay Lobes retreated northward from the coastal zone (Stone et al., 2005). These include the Old Saybrook and Ledyard moraines in Connecticut, which are correlated with the Wolf Rocks and Congdon Hill moraines in Rhode Island, respectively (Figure 1; Boothroyd et al., 1998; Stone et al., 2005). The boulder-lag nature of these moraines indicates that they were affected by meltwater near the ice margin (Stone et al., 2005). Based on their morphostratigraphy, the Connecticut moraines are also tentatively correlated with the Augusta and Sussex recessional moraines in northern New Jersey (Stone and Borns, 1986; Stone et al., 2005; Figure 1). Ice-marginal positions without a moraine are marked by the collapsed ice-contact slopes of individual morphosequences deposited during deglaciation. These features mark the retreat of the ice margin in southern New England and, while they cannot be correlated across valleys for more regional ice positions, they depict systematic retreat of an active ice margin (Koteff and Pessl, 1981; Stone et al., 2005).

To summarize, two large end moraine systems comprise a terminal complex that formed during ice-margin advances as the LIS fluctuated near its maximum extent. The outermost ridges of this complex from northern New Jersey to Nantucket mark the southernmost extent of the LIS, and the innermost ridges of the terminal complex are mapped from the north shore of Long Island to Cape Cod and may be correlated with the Ogdensburg-Culvers Gap moraine in northern New Jersey. Recessional limits in Connecticut and Rhode Island are marked by smaller, discontinuous moraine segments that are starkly different in nature from the moraines of the terminal complex, and which may correlate with recessional moraines north of the Ogdensburg-Culvers Gap moraine in New Jersey.

130

131

132
133
134
135
136
137
138
139
140
141
142

1.1.2 Existing chronologic constraints

Numerous studies have used cosmogenic-exposure dating, radiocarbon dating, optically stimulated luminescence (OSL) dating, and glacial lake sediment records to develop deglacial histories for the LIS in southern New England, New York, and New Jersey (e.g., Dalton et al., 2020; Gorokhovich et al., 2018, Halsted et al., 2022; Peteet et al., 2012; Ridge, 2004; Ridge et al., 2012; Stone and Borns, 1986). The timing of moraine deposition is constrained by bracketing radiocarbon (¹⁴C) ages in pre- and post-glacial sediment (e.g., Stanford et al., 2021; Stone and Borns, 1986; Stone et al., 2005), which we have recalibrated to calendar years BP using the INTCal20 database and CALIB 8.2 (Figure 2; Reimer et al., 2020). Moraines and other ice-marginal deposits dammed lakes fed by glacial melt throughout the region, including Lake Albany, which occupied what is now the Hudson River Valley; glacial Lake Hitchcock, in

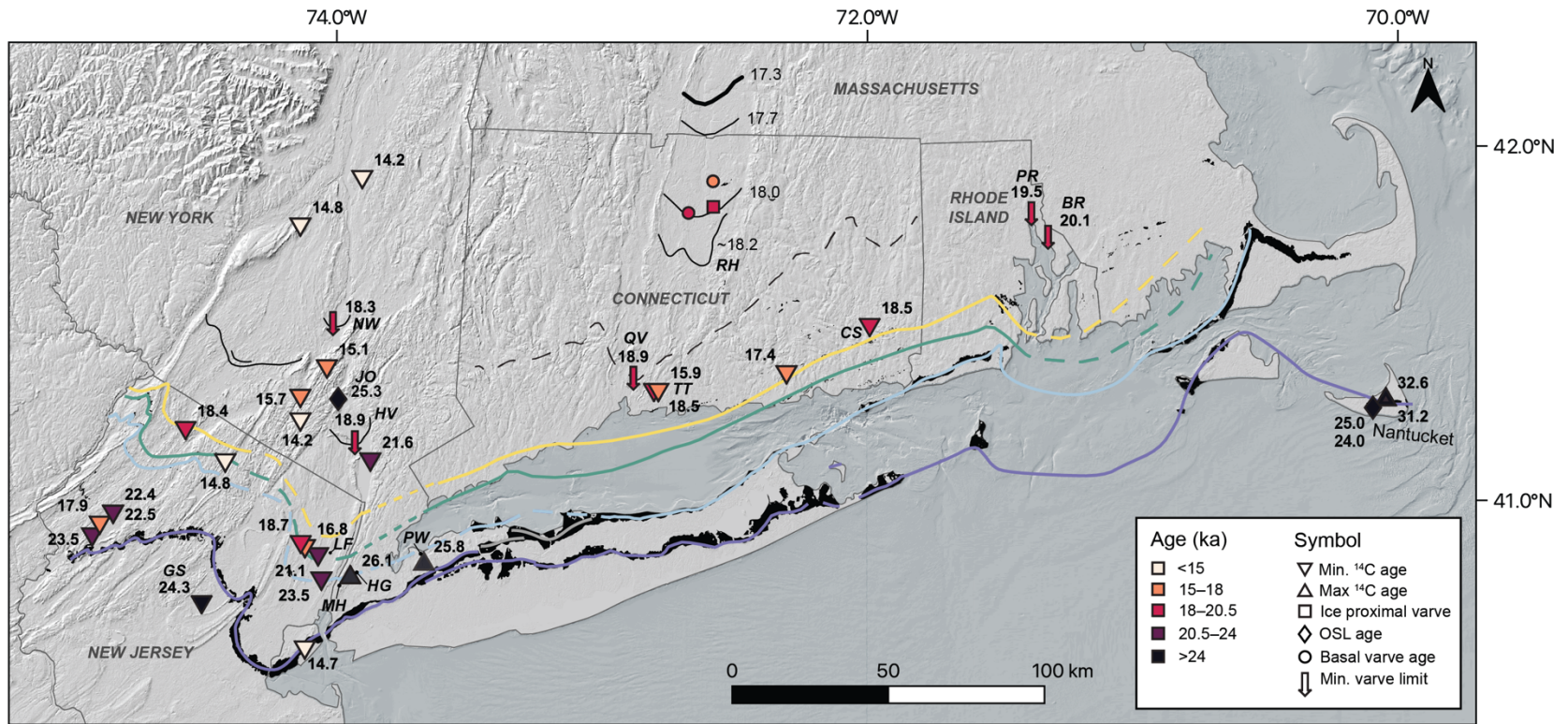


Figure 2 - Previously published chronological constraints based on radiocarbon and glacial varves. Background and ice margin limits same as Figure 1. Ages are discussed and cited in the text. Radiocarbon ages are calibrated to cal. kyr BP. BR = Barrington, RI; CS = Cedar Swamp; GS = Great Swamp; HG = Hell Gate; HV = Haverstraw, NY; JO = Pones Point; LF = Little Ferry varve sequence; MH = Manhattan, New York City; NW = Newburgh, NY; PW = Port Washington; PR = Providence River; QV = Quinnipiac Valley, CT; RH = Rocky Hill; TT = Totoket.

145 what is now the Connecticut River Valley; and lake Narragansett in the Narragansett Bay, Rhode Island (e.g., Antevs,
146 1928, 1922; Oakley and Boothroyd, 2013; Ridge, 2004; Ridge et al., 2012). Annually layered, or varved, sediment
147 throughout the northeast can be aligned across sites to form long varve sequences because the character and thickness
148 of varves deposited in a single year are related to climatic conditions (Antevs, 1928, 1922). These sequences yield a
149 precise chronology of ice margin retreat because (i) the presence of varves indicates ice-free conditions at a given
150 location and (ii) in some cases, a single varve can be traced across sections to its northernmost occurrence, affording
151 a maximum ice margin position for that varve year. The North American Varve Chronology (NAVC) records 5659
152 years of sediment deposition in glacial lakes in New York and New England, including Lakes Hitchcock and Albany,
153 making it the most precise and continuous terrestrial record of LIS retreat through the northeastern United States
154 (Ridge et al., 2012). Varve sequences inboard of LIS moraines also provide minimum limiting ages for those moraines.
155 The NAVC is reported in 'North American Varve Years' numbered 2701-8459, which are calibrated to calendar years
156 by radiocarbon dating of plant macrofossils and other organic material from 54 individual varves throughout the
157 chronology (Ridge et al., 2012). We report NAVC ages in years BP on the Greenland Ice Core timescale (GICC05 yr
158 BP; Andersen et al., 2006) using the offset of 20,925 years (i.e., varve year "0" equals 20,925 years BP) reported in
159 Balco et al. (2021).

160 Absolute ages have been assigned to some of the moraines using cosmogenic exposure dating (Figure 3;
161 Balco et al., 2002; Balco and Schaefer, 2006; Corbett et al., 2017). To integrate the latest developments in cosmogenic-
162 nuclide dating, and to maintain consistency with our new results in this paper, we recalculate published exposure ages
163 using v3 of the online calculator described by Balco et al. (2008), the primary production rate calibration datasets of
164 Borchers et al. (2016) and the scaling method of Lifton et al. (2014; see Methods for further discussion of production
165 rate and scaling method selection). The ages recalculated here therefore differ slightly from the originally reported
166 exposure ages from the same samples given that many of the original publications predate these updated production
167 rate calibration and scaling methods. Finally, we note that while radiocarbon ages and varve years are referenced to
168 1950 CE, the exposure ages are referenced to the time of sample collection (1995–2019 CE). This difference in
169 reference year, however, is negligible for the exposure ages discussed here, which are >18 ka.

170

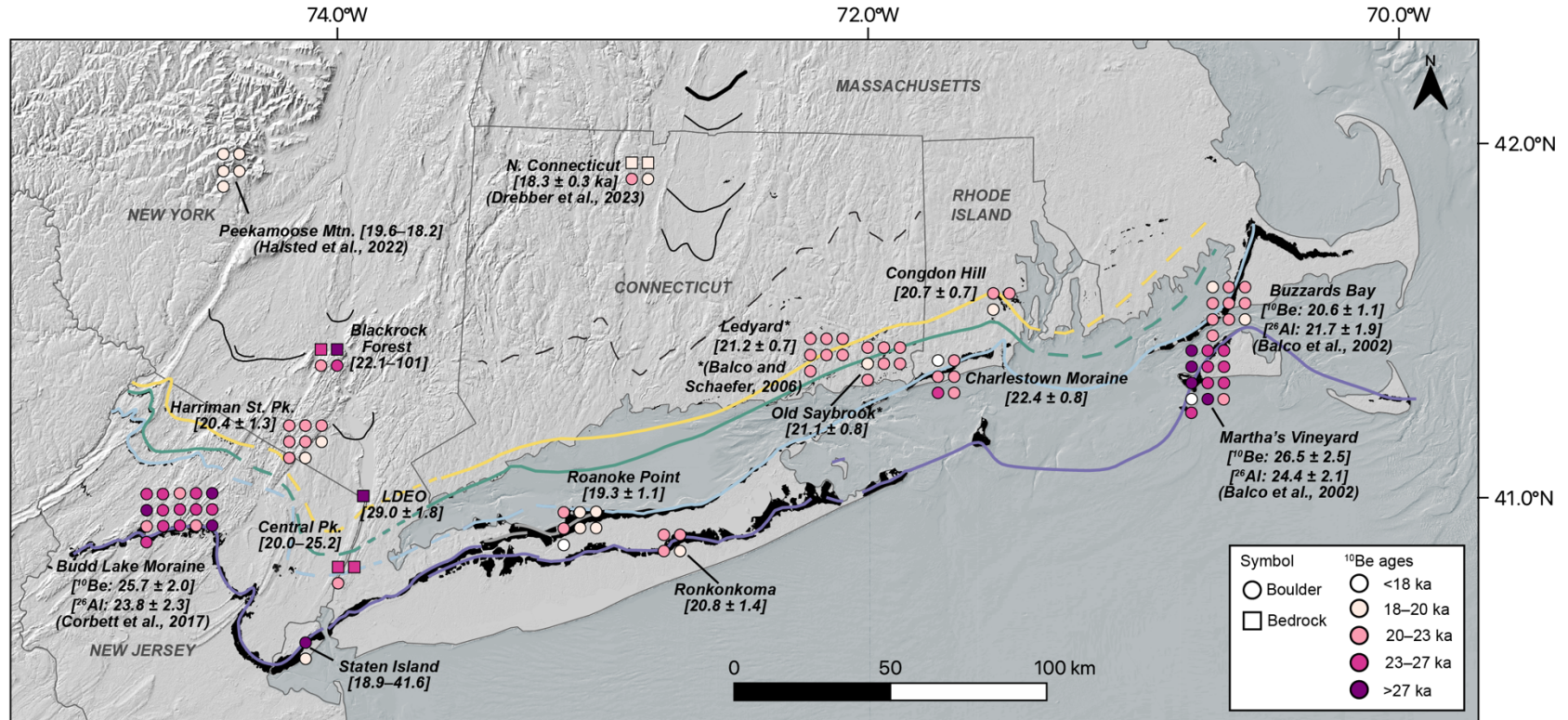


Figure 3 - New and previously published ^{10}Be exposure ages from boulder and bedrock surfaces. Background and ice margin limits same as in Figure 1. Previously published ages are listed with their reference. All are ^{10}Be ages, except where ^{10}Be and ^{26}Al ages are specified. On the Martha's Vineyard and Buzzards Bay moraines, samples with both ^{10}Be and ^{26}Al measurements are colored according to the average of the ^{10}Be and ^{26}Al ages (Balco et al., 2002). Although the Budd Lake moraine samples have both ^{10}Be and ^{26}Al measurements, the symbols are colored only by ^{10}Be age because Corbett et al. (2017) state that many of the ^{27}Al concentrations may be underestimated and therefore exclude the ^{26}Al ages from discussion. The average of the ^{26}Al ages on the Budd Lake moraine is listed for completeness. Where all samples come from the same deposit, the age is listed as mean ± standard deviation, and where samples at a site are not from the same deposit an age range is listed. A full list of sample ages is in Table 1 and moraine ages in Table 2.

173 **Connecticut and Narragansett-Buzzards Bay Lobes:** Previously published radiocarbon and exposure ages
174 constrain the occupation of the outer terminal limit for the Connecticut and Buzzards Bay-Narragansett Lobes to ~27–
175 25 ka. Maximum limiting radiocarbon ages in preglacial deposits near Boston and on Nantucket suggest that the LIS
176 achieved its LGM extent in the east by 32–25 ka (29–21 ¹⁴C kyr BP; n = 3; Figure 2; Oldale, 1982; Schafer and
177 Hartshorn, 1965; Tucholke and Hollister, 1973), which agrees with optically stimulated luminescence (OSL) ages
178 from Nantucket of 24.0 ± 0.9 ka on the oldest moraine and 25.0 ± 0.9 ka on the outboard outwash plain (Stone and
179 Stone, 2019; Rittenour, Stone and Mahan, 2012).

180 ¹⁰Be and ²⁶Al ages on the Martha's Vineyard moraine range from 17.5 to 63.5 ka (n = 12) and from 17.5 to
181 60.5 ka (n = 13), respectively (Figure 3; Balco et al., 2002). Some of these exposure ages, especially those older than
182 the main age population (>30 ka), likely contain ¹⁰Be and ²⁶Al inherited from a previous exposure period (Balco et al.,
183 2002). Production of ¹⁰Be and ²⁶Al attenuates exponentially with depth in rock (Lal, 1991), meaning that subglacial
184 erosion of a few meters during glacial periods strips the surface of cosmogenic nuclides that accumulated during prior
185 exposure (Harbor et al., 2006). Inherited cosmogenic nuclides therefore persist in places where subglacial erosion is
186 insufficient to remove the signature of prior exposure because of minimally erosive (e.g., cold-based) ice, short ice-
187 cover durations, or both (e.g., Briner et al., 2006; Stone et al., 2003; Young et al., 2016). Furthermore, the LIS likely
188 remobilized boulders with significant cosmogenic-nuclide inventories at or near the terminal position as it advanced
189 towards its LGM extent, so it is not surprising that some of the exposure ages on the terminal moraine are older than
190 its true emplacement age. Large end moraines with kame and kettle topography, such as the Martha's Vineyard
191 moraine, also experience permafrost disturbance, which may expose boulders that were previously embedded in the
192 moraine and shielded from the cosmic-ray flux for some time after deposition (Applegate et al., 2010), or shift or
193 rotate boulders so original (upon deposition) top surfaces were not sampled. Exposure ages on exhumed or disturbed
194 (e.g., by agricultural practices and other human activities) boulders are therefore younger than the true emplacement
195 age of the moraine. Excluding exposure ages likely affected by nuclide inheritance or postdepositional disturbance (n
196 = 4), ¹⁰Be ages on the Martha's Vineyard moraine average 26.5 ± 2.5 ka (n = 8; mean ± standard deviation) and ²⁶Al
197 ages average 24.4 ± 2.1 ka (n = 9; Figure 3; Balco et al., 2002; Balco, 2011), and are generally consistent with the
198 maximum-limiting radiocarbon ages in the region and the OSL ages on Nantucket.

199 ¹⁰Be exposure ages on the Buzzards Bay moraine average 20.6 ± 1.1 ka (n = 10) and ²⁶Al ages average 21.7
200 ± 1.9 (n = 10; Balco et al., 2002). The Old Saybrook and Ledyard moraines in Connecticut have ¹⁰Be exposure ages
201 of 21.1 ± 0.8 (n = 7) and 21.2 ± 0.7 ka (n = 7), respectively (Figure 3; Balco and Schaefer, 2006). Thus, although the
202 moraines represent a recessional sequence and were not deposited simultaneously, their ages are indistinguishable
203 within 1σ uncertainty. Postglacial sediment containing tundra vegetation at Cedar Swamp, immediately north of the
204 Ledyard moraine, gives a minimum limiting age for the recessional moraine sequence of 18.5 ± 0.7 ka (mean age ±
205 2σ uncertainty; 15.2 ± 0.3 ¹⁴C kyr BP; McWeeney, 1995; Stone et al., 2005). A radiocarbon age of 18.5 ± 0.3 ka (15.1
206 ± 0.2 ¹⁴C kyr) at Totoket, near New Haven, Connecticut, also provides a minimum limiting age for the Ledyard
207 moraine (Figure 2; Davis et al., 1980; Deevey, 1958).

208 Varve sequences in the region also place minimum age constraints on the recessional moraine sequence. The
209 NAVC in the Connecticut River Valley begins a few kilometers north of Rocky Hill, the spillway for glacial Lake

210 Hitchcock (Figures 1 and 2; Antevs, 1928; Ridge et al., 2012). The Rocky Hill sequence overlaps with a varve section
211 in Newburgh, New York, which together imply that the ice margin had retreated to Newburgh and Rocky Hill by
212 ~ 18.2 ka (varve year 2701; Figure 2; Antevs, 1928, 1922; Balco et al., 2021; Ridge, 2004; Ridge et al., 2012). Several
213 varve sections south of Rocky Hill and Newburgh cannot be correlated with the NAVC and are therefore presumed
214 older, providing minimum estimates for LIS retreat. A ~ 500 yr varve sequence in the Quinnipiac Valley, near New
215 Haven, CT, is correlated with a 700-year sequence in Haverstraw, New York, placing a minimum age for ice-free
216 conditions at Quinnipiac and Haverstraw of >18.9 ka (varve year 2000; Figure 2; Antevs, 1928; Balco and Schaefer,
217 2006; Ridge et al., 2012). Farther east, in the Providence River, Rhode Island, a 600-year varve sequence cannot be
218 correlated with the NAVC. Summing the Providence River sequence with several varve sequences in Connecticut and
219 southern Massachusetts between the base of the NAVC and Providence (including the Quinnipiac/Haverstraw varves),
220 the ice margin must have retreated past Barrington, Rhode Island by ~ 20.1 ka and north of Providence by ~ 19.5 ka
221 (Figures 1 and 2; Oakley and Boothroyd, 2013). Three cosmogenic exposure ages ~ 30 km north of the Rocky Hill
222 Dam average 18.3 ± 0.3 ka, corroborating the deglaciation timing in northern Connecticut (Drebber et al., 2023).

223 The NAVC reveals systematic net ice retreat through New England at $50\text{--}300$ m yr⁻¹ (Ridge et al., 2012),
224 interrupted by relatively minor advances or stillstands at least in the White Mountains and Maine, documented by
225 comprehensive ¹⁴C-based chronologies and ¹⁰Be dating (e.g., Borns et al., 2004; Bromley et al., 2015; Davis et al.,
226 2015; Dorion et al., 2001, Hall et al., 2017; Kaplan, 2007; Koester et al., 2017; Thompson et al., 2017). The position
227 of the retreating ice margin is also marked by annual DeGeer moraines spaced 100 to 300 m apart in northern New
228 England (Sinclair, 2018; Todd, 2007; Wroblewski, 2020). The LIS margin had retreated north of New England by 13.6
229 ka (Ridge et al., 2012), with slightly later retreat or pockets of smaller residual glaciers perhaps lasting only briefly
230 longer in areas of northern Maine (Borns et al., 2004).

231
232 **Hudson Lobe:** Bulk radiocarbon ages from preglacial deposits in Port Washington, New York, and Manhattan, New
233 York, date to 25.8 ± 1.6 ka (21.8 ± 0.8 ¹⁴C kyr BP) and 26.1 ± 0.3 (21.7 ± 0.1 ¹⁴C kyr BP), respectively, giving
234 maximum limiting ages for the Hudson Lobe terminal moraine (Figure 2; Schuldenrein and Aiuvalasit, 2011; Sirkin
235 and Stuckenrath, 1980). This agrees with an OSL age of 25.3 ± 7.4 ka on proglacial deposits in Jones Point, New
236 York, associated with the advance of the Hudson Lobe (Gorokhovich et al., 2018). A bulk radiocarbon age of $24.3 \pm$
237 1.1 ka (20.2 ± 0.5 ¹⁴C kyr BP) from an LGM varve sequence at Great Swamp, New Jersey, provides a minimum
238 limiting age for the Budd Lake moraine in New Jersey (Figure 2; Reimer, 1984; Stanford et al., 2021). Boulders a few
239 km inboard of the Budd Lake moraine have ¹⁰Be ages of 25.7 ± 2.0 ka ($n = 16$) and ²⁶Al ages of 23.8 ± 2.3 ka ($n =$
240 16), although the original publication excludes the ²⁶Al ages from discussion given evidence that the ²⁷Al
241 concentrations were underestimated (Figure 3; Corbett et al., 2017). Together, the existing chronological constraints
242 suggest that the Hudson Lobe of the LIS reached its southernmost extent by $\sim 25\text{--}26$ ka and abandoned that limit by
243 ~ 24 ka (Corbett et al., 2017; Stanford et al., 2021).

244 The varves at Haverstraw, New York, place a minimum limiting age of 18.9 ka on the Ogdensburg-Culver
245 Gap, Augusta and Sussex recessional moraines in northern New Jersey (Ridge et al., 2012). A floating varve sequence
246 at Little Ferry in Teterboro, NJ, comprises 1100 glacial varves that must be older than the Haverstraw sequence and

247 1430 postglacial varves that may overlap with the Haverstraw varves (Antevs, 1928, Stanford et al., 2012). The Little
248 Ferry varves therefore place a minimum limit of ~20 ka on the Augusta position (18.9 + 1.1 kyr; Figure 2). A recent
249 compilation of chronologic constraints in northern New Jersey, places the base of the Little Ferry varve sequence at
250 ~23.5 ka based on a nearby bulk radiocarbon age (Stanford et al., 2021). Considering these varve sequences alongside
251 additional radiocarbon ages in northern New Jersey, Stanford et al. (2021) hypothesized that the Hudson Lobe
252 abandoned the terminal moraine at ~24 ka and retreated to the position of the Sussex moraine, the innermost of the
253 northern New Jersey recessional moraines, by ~23.5 ka. Based on their revised chronology, Stanford et al. (2021)
254 suggested that the Connecticut recessional moraines (Ledyard and Old Saybrook) may correlate with the New
255 Hampton and Pellets Island moraines in New York, rather than the northern New Jersey recessional sequence.

256 The earliest post-glacial radiocarbon ages on plant macrofossils in lake and bog sediment throughout the
257 region date to ~14–18.5 ka (Figure 2; Davis et al., 1980; Deevey, 1958; McWeeney, 1995; Stone et al., 2005; Peteet
258 et al., 2012). These dates provide further minimum-limiting ages for the moraine sequences discussed here. The
259 abundance of macrofossils dating to ~14–16 ka, in addition to the fact that most ages older than 16 ka come from bulk
260 sediment that are more likely to contain old carbon, has been used to argue that the LIS abandoned its LGM limit ~14–
261 16 ka (Peteet et al., 2012), and thus ~8–10 ka later than is indicated by the exposure-age and radiocarbon datasets
262 presented and compiled here.

263 **2. Geomorphology and study areas**

264 The Connecticut and Narragansett-Buzzards Bay Lobes exhibit exceptionally well preserved moraines that
265 afford an opportunity to constrain the regional timing of the LGM and its culmination. Below, we describe the
266 geomorphic settings and sample locations for 40 new exposure ages from the Connecticut and Narragansett-Buzzards
267 Bay Lobe in Long Island, New York and Rhode Island, as well as from the Hudson Lobe to the west.

268 **2.1 Connecticut and Narragansett Lobes**

269 **2.1.1 Long Island, New York**

270 Long Island is a large (~200 km long and 35 km wide), densely populated island in the New York
271 Metropolitan area that extends from Brooklyn, New York City to its eastern extents at Montauk and Orient Point
272 (Figure 1). The Island comprises tills and outwash plains associated with the southernmost extent of the LIS at the
273 LGM, and its topography is defined by several prominent moraine ridges (>60 m relief, at points), including the
274 Ronkonkoma, Harbor Hill and Roanoke Point moraines (Figure 1; Fuller, 1914; Sirkin, 1982; Sirkin and Stuckenrath,
275 1980). The Ronkonkoma moraine is the stratigraphically oldest (southernmost) associated with the Connecticut Lobe
276 of the LIS and extends E-W from the hamlet of Jericho in west-central Long Island to Montauk, forming the South
277 Fork of Long Island. The moraine ridge comprises discontinuous kame deposits and thrust sheets overlain by thin,
278 sandy till and bisected by outwash-filled valleys (Cadwell, 1989; Sirkin 1982). The easternmost point of the
279 Ronkonkoma moraine at Montauk Point is correlated with the outer terminal moraine positions on Block Island,
280 Martha's Vineyard, and Nantucket (Stone and Borns, 1986; Sirkin, 1976). Although boulders ideal for surface

281 exposure dating were difficult to locate on the Ronkonkoma moraine, we sampled four medium-sized (~1 m height)
282 graniod boulders near Manorville, NY (Figure S1).

283 The Harbor Hill moraine was originally correlated with the New Jersey terminal position, mapped as
284 extending from Staten Island and across the north shore of Long Island, crosscutting the Ronkonkoma moraine near
285 Jericho, New York (Fuller, 1914; Figure 1). Yet, updated models of Long Island glaciation demonstrate that the
286 classical Harbor Hill moraine comprises several segments that may have been deposited asynchronously (Sirkin, 1982;
287 Stone and Borns, 1986). Here, the term Harbor Hill moraine refers to the segment extending from the confluence with
288 the Ronkonkoma moraine through Staten Island, which represents the terminal limit of the Hudson Lobe in western
289 Long Island (Figure 1), while the Northport Stony Brook moraine segments northeast of the confluence with the
290 Ronkonkoma moraine are considered younger positions (Sirkin, 1982; Stone and Borns 1986). A stratigraphic section
291 in Port Washington, New York, reveals that the Harbor Hill moraine is characterized by ablation till up to 10 m thick
292 overlying thrust sheets of stratified drift containing dislocated preglacial deposits, suggesting it formed during a
293 readvance (Mills and Wells, 1974; Oldale and O'Hara, 1984). Several additional moraine segments are mapped north
294 of the Ronkonkoma ice-margin position in eastern Long Island (Sirkin 1982; Sirkin, 1998), which are not discussed
295 further here.

296 The Roanoke Point landform is the innermost Connecticut Lobe moraine on Long Island. It appears to
297 crosscut the Stony Brook moraine segment near Port Jefferson, New York, extending east to Orient Point, forming
298 the North Fork of Long Island (Figure 1; Cadwell, 1989; Sirkin, 1982). The moraine consists of till over deformed
299 outwash (Sirkin, 1982). Glaciotectonic structures, such as imbricated thrust sheets and dislocated strata, within the
300 moraine stratigraphy indicate that the moraine was likely deposited during a readvance of the ice margin, rather than
301 a representing a standstill (Oldale and O'Hara, 1984; Boothroyd and Sirkin, 2002). The Roanoke Point moraine is
302 correlated with the Sands Point moraine to the west, deposited by the Hudson Lobe, and tentatively correlated with
303 the Odgensburg-Culvers Gap moraine in northwest New Jersey (Figure 1; Section 1.1.1; Stanford, 2010, 1993;
304 Stanford et al., 2021; Stanford and Harper, 1991; Stone et al., 2002, 1995). We sampled seven large (>1 m tall, with
305 some as tall as 4 m) erratic boulders on or near the Roanoke Point moraine in the vicinity of Port Jefferson, New York,
306 and Stony Brook University (Figure 4; Figure S1).

307 Mapping and sampling of the Long Island moraines was undertaken through the Lamont-Doherty Earth
308 Observatory Undergraduate Student Summer Intern Program between 2002-2006. Original field observations from
309 2006 note that one sample, LI-9, is located in a topographic depression, and may have been exhumed or toppled after
310 deposition. Upon further inspection in 2023, many of the samples collected from the Roanoke Point moraine are
311 located in topographic low points, and only LI-1 and LI-8 were taken from local high points where boulders were less
312 likely to have been affected by postdepositional processes (Figure S1).

313



Figure 4 - Representative sampling locations for surface exposure dating. LI-3: Large boulder sampled in an urban setting of the Roanoke Point moraine on Long Island. The sizable boulder is slightly off the moraine crest (in the background), not located on a local high point and may have experienced postdepositional disturbance. GB2002-CH-4: stable boulder on the Charlestown moraine. Ledyard Moraine: interlocked boulders of the Ledyard moraine in Connecticut. Harriman State Park: Interlocked boulders forming an ice-marginal boulder deposit.

314
315
316
317
318
319
320
321
322
323
324
325

2.1.2 Rhode Island

Three ice marginal positions in southern Rhode Island are marked by the Charlestown, Wolf Rocks and Congdon Hill moraines. The stratigraphically oldest is the Charlestown moraine, which is part of the Roanoke Point - Fishers Island - Charlestown - Buzzards Bay limit (Figure 1; Kaye, 1960; Upham, 1879). The moraine is ~30 km by 0.5–3 km wide, rising as much as 30 m above the surrounding topography (Kaye, 1960). It is composed of a mixture of diamict and glaciotectonically displaced stratified deposits (sand and gravel), suggesting it formed during a readvance, with numerous large boulders at the surface (Boothroyd et al., 1998; Boothroyd et al., 2002; Oldale and O’Hara, 1984; Schafer, 1965). The Wolf Rocks boulder moraine, which we did not sample, is inboard of the Charlestown moraine and is correlated with the Old Saybrook recessional moraine in Connecticut (Stone et al., 2005). The Congdon Hill moraine is the innermost recessional moraine in Rhode Island and is correlated with the Ledyard recessional moraine in Connecticut to the west (Boothroyd and Sirkin, 2002; Stone et al., 2005). This hummocky

326 moraine ridge is 6 km long and 3–20 m in height and comprises boulders and sandy till, with numerous large boulders
327 near the moraine crest (Stone, 2014).

328 We collected six samples on the Charlestown moraine, and three samples on the Congdon Hill moraine, all
329 of which were from large (>1 m) boulders (Figure 4; Figure S2). Field observations note that sample GB2002-CH-1
330 on the Charlestown moraine was collected from a boulder that had collapsed into a gravel pit. Although it appeared
331 that its original position could be reconstructed from weathering characteristics and other evidence, this could not be
332 verified.

333

334 **2.2 Hudson Lobe**

335 The Hudson Lobe of the LIS deposited a NE-SW trending moraine on Staten Island that correlates with the
336 terminal moraines on Long Island to the east (Figure 1; Cadwell, 1989) and in northern New Jersey to the west (Stone,
337 2002). The hummocky moraine is 0.5–4 km wide by 20 km long, comprising primarily reddish-brown, clayey tills
338 that are up to ~45 m thick (Soren, 1988). Boulders are rare on the moraine crest (Soren, 1988), but we found two
339 granite boulders suitable to sample (Figure S3).

340 We also present new exposure ages from several locations in the Lower Hudson Valley at Central Park in
341 New York City, Lamont-Doherty Earth Observatory (LDEO), Harriman State Park, and Black Rock Forest (Figure
342 1). Glacially molded outcrops of Manhattan Schist in Central Park, New York City, 25 km north of the terminal
343 moraine, are sparsely overlain by erratic boulders sourced from pegmatitic granites that outcrop ~15 km north of
344 Central Park near the Bronx Zoo (Brock and Brock, 2001; Jaret et al., 2021; Taterka, 1987). We sampled two quartz
345 veins within Manhattan Schist, one from Umpire Rock at the southwest corner of Central Park, and one in the
346 northwest corner of the park, as well as a boulder from the southeast corner of the Sheep Meadow (Collins, 2005). At
347 LDEO, ~50 km north of the terminal limit, we collected a single sample for surface exposure dating from the Palisades
348 diabase. At Harriman State Park, ~70 km north of the terminal moraine, we sampled eight large (generally >2 m tall)
349 gneiss or granitoid boulders from an area with a large concentration of erratics, representing a local ice-marginal
350 deposit, in an area near two large boulders called the Grandma and Grandpa Rocks (Figure 4). The erratics are perched
351 on bedrock, or on top of thin till veneer. Finally, at Black Rock Forest, ~90 km north of the outer terminal limit, we
352 collected three samples of glacially eroded gneissic bedrock and two samples from large (>2 m tall) granite boulders.

353 **3 Methods**

354 Samples for surface exposure dating from the upper surfaces of bedrock and erratic boulders were collected
355 between 2002 and 2006 using the drill-and-blast method of (Kelly, 2003) and/or hammer and chisel. We collected one
356 replicate sample at Black Rock Forest (BRF-19-01) in 2019. At each site, we measured topographic shielding using a
357 clinometer and recorded the sample location and elevation using handheld GPS, except for the samples from Rhode
358 Island for which elevations were measured by barometer traverse from the nearest USGS benchmark. Samples were
359 processed at the Lamont-Doherty Earth Observatory cosmogenic dating laboratory following established procedures
360 for isolating quartz and extracting beryllium (e.g., Schaefer et al., 2009). $^{10}\text{Be}/^9\text{Be}$ ratios were measured at the Center

361 for Mass Spectrometry at Lawrence Livermore National Laboratory (LLNL-CAMS) between August 2005 and July
362 2007, with one additional measurement in July 2019. Prior to 2007, samples were measured relative to the KNSTD
363 standard with a $^{10}\text{Be}/^9\text{Be}$ ratio of 3.11×10^{-12} (Nishiizumi, 2002). Measurements in 2007 or later were made relative
364 to the 07KNSTD standard with a $^{10}\text{Be}/^9\text{Be}$ ratio of 2.85×10^{-12} (Nishiizumi et al., 2007), which is taken into account
365 for our ^{10}Be age calculations (Balco et al., 2008). ^{10}Be concentrations ranged from 5.61×10^4 to 6.17×10^5 with
366 analytical uncertainty of 2–9%. Blank corrections, calculated by subtracting the average number of ^{10}Be atoms from
367 blanks processed in each sample batch, ranged from <0.5–12%, with the majority of blank corrections being <2%
368 (Table S1). Reported uncertainties in ^{10}Be concentrations include analytical errors, blank errors, and uncertainties
369 related to the ^9Be concentration (1.5%) propagated in quadrature.

370 Apparent ^{10}Be exposure ages are calculated using Version 3 of the online exposure calculator described by
371 Balco et al. (2008) and subsequently updated, with all information needed to calculate exposure ages available at
372 <https://version2.ice-d.org/laurentide/publication/1187/>. Here, “apparent” exposure ages refer to the calculated surface
373 age assuming a single period of exposure with no erosion or burial. We note that including the effects of subaerial
374 rock erosion or snow cover would make the ages presented here slightly older. Since the publication of the first
375 exposure age chronologies in southern New England, efforts have been made to better estimate cosmogenic-nuclide
376 production rates at sites with independent age control (e.g., Balco et al., 2009; Kaplan et al., 2011; Putnam et al., 2019;
377 Young et al., 2013). Of particular relevance here, Balco et al. (2009) established a regional ^{10}Be production rate
378 calibration dataset for northeastern North America (NENA) using ^{10}Be measurements at independently dated sites in
379 New England, most of which are part of the NAVC, and on Baffin Island, Canada. In an effort to synthesize several
380 new and existing production rate datasets, Borchers et al. (2016) describe “primary” production rate datasets for ^{10}Be
381 and ^{26}Al (among other nuclides), which includes sites that range in latitude and elevation, but does not include
382 calibration sites from NENA. As of this writing, the ^{10}Be reference production rates calculated using the NENA and
383 Borchers et al. (2016) datasets differ by only ~1.5% (reference production rates calculated in the online production
384 rate calculator described by Balco et al. (2008) and subsequently updated
385 (http://hess.ess.washington.edu/math/v3/v3_cal_in.html; last access January 26, 2023). Given the similarity of these
386 two production-rate datasets, we here employ the ^{10}Be and ^{26}Al production rates of Borchers et al. (2016) to avoid
387 circularity when discussing the agreement of the exposure age chronology with the NAVC. In addition, time-
388 dependent production rate scaling frameworks, which account for changes in the geomagnetic field (and therefore
389 cosmic ray flux to the Earth’s surface), have been more widely adopted. The LGM moraines discussed here have
390 exposure ages older than those at the production rate calibration sites (Balco et al., 2009; Borchers et al., 2016), so
391 employing time dependent scaling methods may produce more accurate exposure ages. Therefore, we discuss
392 exposure ages calculated using the primary production rate calibration dataset of Borchers et al. (2016) and time-
393 dependent “LSDn” production rate scaling method of Lifton et al. (2014), although also provide ages calculated using
394 the NENA production rate calibration dataset of Balco et al. (2009; NENA) and non-time-dependant “St” scaling (Lal,
395 1991; Stone, 2000) in Tables S2 and S3. We recognize that the choice of scaling method affects moraine absolute
396 exposure ages by up to ~5% (Table 2), but emphasize this is within the uncertainty of many moraine ages, and does
397 not affect the calculated rates of net retreat between moraines nor our conclusions.

398 **4 Results**

399 Exposure ages from Long Island, New York, and Rhode Island, which are presented in Table 1 and Figure 3,
400 are relevant to the glacial history of the Connecticut and Narragansett-Buzzards Bay Lobes of the LIS. Ages on the
401 Ronkonkoma moraine range from 19.1 to 22.4 ka, with an average of 20.8 ± 1.4 ka (average \pm SD; $n = 4$). Boulders
402 on the Roanoke Point moraine range in age from 18.2 to 20.9 ka, averaging 19.3 ± 1.1 ka ($n = 6$), with one outlier
403 that is 14.2 ± 0.6 ka. In Rhode Island, six boulders on the Charlestown moraine have exposure ages that range from
404 21.8 to 23.7 ka, with one outlier (GB2002-CH-1) excluded because field observations indicated the boulder may not
405 have been in its original position (Section 2.1.2), as confirmed by an exposure age (17.4 ± 1.6 ka) younger than the
406 main population of ages on this moraine. The average age of the Charlestown moraine is 22.4 ± 0.8 ka ($n = 5$).
407 Boulders on the Congdon Hill moraine range in age from 20.0 to 21.3 ka, and average 20.7 ± 0.7 ka ($n = 3$).

408 Additional exposure ages west of Long Island in southern New York, pertain to the Hudson Lobe of the LIS
409 (Figure 3). On Staten Island, two boulders yield ^{10}Be ages of 41.6 ± 2.4 and 18.9 ± 2.1 ka. In Central Park, Manhattan,
410 two ^{10}Be ages from bedrock samples are 25.0 ± 0.7 and 23.2 ± 0.8 and an erratic boulder from Sheep Meadow yields
411 an age of 20.0 ± 0.7 ka. A single ^{10}Be age on bedrock at the Lamont-Doherty Earth Observatory is 29.0 ± 1.8 ka.
412 Samples from the ice-marginal deposit in Harriman State Park range in age from 18.7 to 22.8 ka, averaging 20.4 ± 1.3
413 ka ($n = 8$). Finally, three bedrock samples at Black Rock Forest date to 25.0 ± 0.7 , 102 ± 3 , and 101 ± 3 ka (the latter
414 two bedrock samples are from the same outcrop), and two boulder samples date to 23.7 ± 0.8 and 22.1 ± 0.8 ka.

415
416
417
418
419
420
421
422
423
424
425
426
427
428
429
430
431
432

Table 1 - New ^{10}Be exposure ages in southern New England and New York. All ages calculated using the primary production rate dataset of Borchers et al. (2016)

Sample ID	Sample type	^{10}Be Age LSDn scaling (yrs)	^{10}Be age internal error LSDn Scaling (yrs)	^{10}Be Age St scaling (yrs)	^{10}Be age internal error St Scaling (yrs)	Included in landform age reported in Table 2?
Connecticut Lobe						
<i>Ronkonkoma Moraine, Long Island, NY</i>						
LI-10	boulder	22400	800	21600	700	yes
LI-11	boulder	20700	700	19700	600	yes
LI-13	boulder	21100	700	20100	700	yes
LI-14	boulder	19100	800	18000	700	yes
 <i>Roanoke Point Moraine, Long Island, NY</i>						
LI-1	boulder	20100	1000	19100	900	yes
LI-3	boulder	19800	600	18800	600	yes
LI-4	boulder	18300	600	17300	500	yes
LI-6A	boulder	18900	700	18000	600	yes
LI-6B	boulder	18300	500	17300	500	yes
LI-7	boulder	18200	600	17200	500	yes
LI-8	boulder	20900	700	20000	600	yes
LI-9	boulder	14200	600	13300	500	no

Table 1 - Cont'd.

Sample ID	Sample type	¹⁰Be Age LSDn scaling (yrs)	¹⁰Be age internal error LSDn Scaling (yrs)	¹⁰Be Age St scaling (yrs)	¹⁰Be age internal error St Scaling (yrs)	Included in landform age reported in Table 2?
<i>Charlestown Moraine, Rhode Island</i>						
GB2002-CH-1	boulder	17400	1600	16500	1500	no
GB2002-CH-2	boulder	21800	800	21100	700	yes
GB2002-CH-3	boulder	22200	1100	21500	1100	yes
GB2002-CH-4	boulder	22500	800	21800	700	yes
GB2002-CH-5	boulder	23700	1000	23100	1000	yes
GB2002-CH-6	boulder	21900	1000	21100	1000	yes
<i>Narragansett-Buzzards Bay Lobe</i>						
<i>Congdon Hill Moraine</i>						
GB2002-CO-1	boulder	21400	700	20600	700	yes
GB2002-CO-2	boulder	20900	1000	20100	1000	yes
GB2002-CO-3	boulder	20000	1200	19100	1100	yes
<i>Hudson Lobe</i>						
<i>Harbor Hill Moraine, Staten Island, NY</i>						
SI-1	boulder	41600	2400	40700	2400	n/a
SI-3	boulder	18900	2100	17800	2000	n/a

Table 1 - Cont'd.

Sample ID	Sample type	¹⁰Be Age LSDn scaling (yrs)	¹⁰Be age internal error LSDn Scaling (yrs)	¹⁰Be Age St scaling (yrs)	¹⁰Be age internal error St Scaling (yrs)	Included in landform age reported in Table 2?
<i>Central Park, Manhattan, NY</i>						
UDP-2	bedrock	25000	700	24200	700	n/a
UDP-3	bedrock	23200	800	22300	800	n/a
UDP-4	boulder	20000	700	19000	700	n/a
<i>Lamont-Doherty Earth Observatory, Palisades, NY</i>						
LDEO-1	bedrock	29000	1800	28200	1700	n/a
<i>Harriman State Park, New York</i>						
HSP-1	boulder	20600	700	19700	700	yes
HSP-2a	boulder	20300	700	19400	600	yes
HSP-3	boulder	21500	700	20700	600	yes
HSP-4	boulder	20300	800	19400	700	yes
HSP-06-01	boulder	22800	800	22000	800	yes
HSP-06-04	boulder	19100	700	18200	700	yes
HSP-06-05	boulder	20200	600	19300	600	yes
HSP-06-06	boulder	18700	700	17800	700	yes

Table 1 - Cont'd

Sample ID	Sample type	¹⁰ Be Age LSDn scaling (yrs)	¹⁰ Be age internal error LSDn Scaling (yrs)	¹⁰ Be Age St scaling (yrs)	¹⁰ Be age internal error St Scaling (yrs)	Included in landform age reported in Table 2?
<i>Black Rock Forest</i>						
BRF-1	bedrock	25000	700	24400	600	n/a
BRF-2	bedrock	102400	2900	101400	2900	n/a
BRF-3	boulder	22100	800	21500	800	n/a
BRF-4	boulder	23700	800	23100	800	n/a
BRF-19-01	bedrock	101100	3000	99900	3000	n/a

434

435

436 **5 Discussion**

437 The dataset of new and previously reported exposure ages spans the LGM (~26–19 ka), providing insight
 438 into the timing of the LIS maximum extent, the LGM duration, and implications for onset of initial retreat in southern
 439 New England and New York. We assess the exposure age chronology in more detail to establish an age for each ice
 440 limit, present estimates for average retreat rates through the study area and place the moraine chronology in a climatic
 441 context.

442 **5.1 Moraine ages**443 **5.1.1 Connecticut and Narragansett-Buzzards Bay Lobes**

444 The cosmogenic-nuclide chronology for the Connecticut and Narragansett-Buzzards Bay Lobes agrees with
 445 limiting age constraints from radiocarbon and glacial lake varves in the region (Figure 2; Figure 5), including for the
 446 timing of the LGM and onset of ice recession. The ¹⁰Be (26.5 ± 2.5 ka) and ²⁶Al ages (24.4 ± 2.1 ka) on the Martha's

447 Vineyard moraine agree within uncertainty with maximum-limiting radiocarbon ages in Port Washington, New York
448 Nantucket, MA, and near Boston, MA, as well as with OSL ages on Nantucket, which together suggest that the
449 southeastern LIS reached its maximum LGM extent by ~32.4–25.6 ka (Section 1.1.2; Balco et al., 2002; Oldale, 1982;
450 Rittenour, Stone and Mahan, 2012; Schafer and Hartshorn, 1965; Stone and Stone, 2019; Tucholke and Hollister,
451 1973). The Ledyard moraine (21.2 ± 0.7 ka; Balco and Schaefer, 2006) and Congdon Hill moraine (20.7 ± 0.7 ka), the
452 innermost recessional moraines discussed here, are slightly older than minimum-limiting ages for these moraines
453 placed by the varve sequences in the Quinnipiac Valley (18.9 ka; Ridge et al., 2012) and the Providence River (20.1
454 ka; Oakley and Boothroyd, 2013; Section 1.1.2).

455 Average exposure ages for each of the Connecticut and Narragansett-Buzzards Bay moraines are generally
456 in stratigraphic order, with the terminal limit being ~24.5–26.5 ka, the Roanoke Point-Charlestown-Buzzards Bay
457 limit being ~19.5–22.5 ka, and the inner limits in Connecticut and Rhode Island being ~20.5–21 ka (Table 2, Figure
458 6). Upon closer inspection, however, the average exposure ages on the Ronkonkoma moraine (20.8 ± 1.4), Roanoke
459 Point moraine (19.3 ± 1.1 ka) and Buzzards Bay moraine (21.2 ± 1.6 ka; Balco et al., 2002) are slightly younger than
460 those of stratigraphically equivalent (Charlestown) and/or inboard (Old Saybrook, Ledyard, and Congdon Hill)
461 moraines (Figure 6), although the age distributions on equivalent ice-margin limits overlap (Table 3; Figures 7). It is
462 not required that stratigraphically equivalent moraine segments are exactly the same age, as it is possible that the
463 timing of moraine emplacement was spatially variable across the region because of long occupation times and/or
464 asynchronous abandonment of the large moraine belts. Yet, it is expected that outboard moraines are older than those
465 inboard, so the apparent departure of average moraine age from stratigraphic ordering can be explained if i) the average
466 ages of the Connecticut and Rhode Island moraines are erroneously old due to nuclide inheritance, and/or ii) the
467 average ages from the Ronkonkoma, Roanoke Point and Buzzards Bay moraines are spuriously young because at least
468 some boulders were affected by postdepositional disturbance.

469 We find it unlikely that the boulders on the Charlestown, Old Saybrook, Ledyard and Congdon Hill moraines
470 contain significant inherited ^{10}Be . ^{10}Be , like most cosmogenic nuclides, is produced by neutron spallation and muon
471 interactions. Spallation dominates production at the Earth's surface and decreases rapidly with depth at an attenuation
472 length of ~160 g cm⁻² at mid-latitudes. Muon interactions account for ~2% of cosmogenic-nuclide production at the
473 Earth's surface but continue to tens of meters depth in rock, comprising the majority of ^{10}Be production below ~2 m
474 depth (Lal, 1991; Balco, 2017). Cosmogenic-nuclide inheritance is most often observed in places where subglacial
475 erosion is low, such as places with cold-based ice, and is generally more pervasive on bedrock surfaces than boulders
476 that have been entrained in ice (e.g., Stone et al., 2003; Young et al., 2016). The distribution of boulder exposure ages
477 on moraines where at least some boulders exhibit inheritance tend to skew old (Applegate et al., 2010), as is the case
478 on the Martha's Vineyard moraine. The distribution of exposure ages on the Connecticut and Rhode Island moraines,
479 however, are normal (Table 2; Figure 6), making the presence of inherited spallation-produced ^{10}Be highly unlikely
480 in the sampled boulders. Although muon-produced ^{10}Be accumulates slowly (< 0.1 atom g⁻¹ yr⁻¹), ^{10}Be builds to
481 measurable concentrations even at several meters depth when rock is exposed for the majority of a glacial cycle, as
482 are landscapes peripheral to the LGM ice sheets. Recent work demonstrates that moraine and erratic boulders near the
483 LGM limit may therefore contain several-thousand-years' worth of muon-produced ^{10}Be in excess of the deposition

484 age even when plucked from rock ~2–6 m below the formerly exposed surface (Briner et al., 2016b; Halsted et al.,
 485 2023). Yet, it is unlikely that all boulders on these moraines, which exhibit an abundance of large boulders (1–2 m;
 486 Figure 4), were sourced from the same depth in

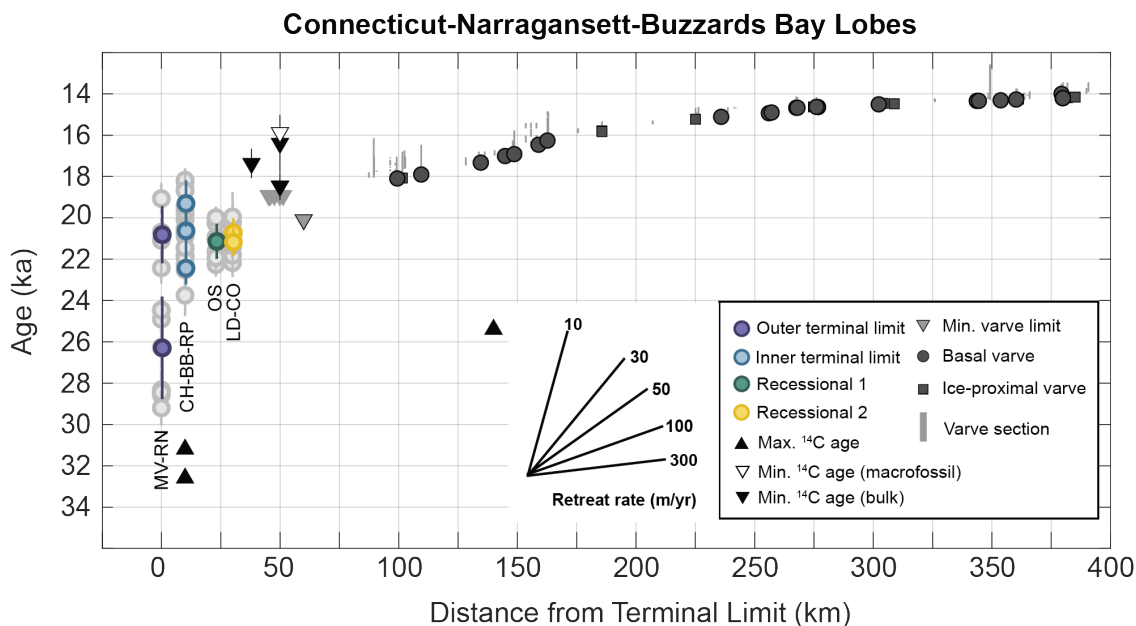


Figure 5 - Time distance diagram for the Connecticut-Narragansett-Buzzards Bay Lobes of the LIS based on the exposure age, radiocarbon, and varve chronologies. Only ¹⁰Be ages are shown for simplicity. Individual boulder ages are shown as light gray circles and average moraine ages are colored as in Figure 1. Moraine names indicated below each limit in order of oldest to youngest. MV = Martha’s Vineyard Moraine, RN = Ronkonkoma Moraine, CH = Charlestown Moraine, BB = Buzzard’s Bay Moraine, RP = Roanoke Point Moraine, OS = Old Saybrook Moraine, LD = Ledyard Moraine, CO = Congdon Hill moraine. Inset shows the slopes associated with various retreat rates.

487

Table 2 - Moraine ages and statistics.

Moraine name	Distance from terminal moraine¹	Boulder count (samples excluded)	LSDn Exposure age (yrs)²	1σ error in LSDn Exposure age (yr)²	St Exposure age (yrs)²	1σ error in St Exposure age (yr)²	Coefficient of Variance (%)	Reduced χ^2	Reference
<i>Outer Terminal Limit</i>									
Budd Lake Moraine	0	16 (0)	25.7	2.0	24.9	2.1	8%	6.14	Corbett et al., 2017
Ronkonkoma Moraine	0	4 (0)	20.8	1.4	19.9	1.4	7%	3.36	This study
Martha's Vineyard Moraine	0	8 (4)	25.4	2.5	24.9	2.6	8%	6.09	Balco et al., 2002
<i>Inner Terminal Limit</i>									
Roanoke Point Moraine	10 to 25	6 (1)	19.3	1.1	18.3	1.1	6%	3.33	This study
Charlestown Moraine	28	5 (1)	22.4	0.8	21.7	0.8	4%	0.68	This study
Buzzards Bay Moraine	8 to 30	10 (0)	21.2	1.6	20.6	1.7	8%	2.00	Balco et al., 2002
Roanoke Point-Charlestown-Buzzards Bay Combined	8 to 30	12 (11)	22.2	0.8	21.6	0.8	3%	1.00 ⁴	Balco et al., 2002 and this study

Table 2 – Cont'd.

Moraine name	Distance from terminal moraine¹	Boulder count (samples excluded)	LSDn Exposure age (yrs)²	1σ error in LSDn Exposure age (yr)²	St Exposure age (yrs)²	1σ error in St Exposure age (yr)²	Coefficient of Variance (%)	Reduced χ^2	Reference
<i>Recessional Limit 1</i>									
Old Saybrook Moraine	35 to 43	7 (0)	21.1	0.8	20.4	0.9	4%	2.10	Balco and Schaefer, 2006
<i>Recessional Limit 2</i>									
Ledyard Moraine	44 to 46	7 (0)	21.2	0.7	20.4	0.7	3%	1.21	Balco and Schaefer, 2006
Congdon Hill Moraine	50	3 (0)	20.7	0.7	19.9	0.7	3%	0.59	This study
Ledyard-Congdon Hill Combined	44 to 50	10 (0)	21.0	0.7	20.2	0.7	3%	0.91	This study
<i>Minimum Limit</i>									
Harriman State Park (ice-marginal deposit)	40 to 50	8 (0)	20.4	1.3	19.6	1.3	6%	2.92	This study

¹Measured parallel to transect in Figure 1.

²All ages calculated using the primary production rate dataset of Borchers et al. (2016). Ages calculated using the NENA production rate dataset of Balco et al. (2009) shown in Table S3. All ages are from ¹⁰Be, except for on the Martha's Vineyard and Buzzards Bay moraines, for which ²⁶Al and ¹⁰Be measurements are reported and discussed in the original publication (Balco et al., 2002). ²⁶Al measurements are also reported for the Budd Lake moraine, but Corbett et al. (2017) do not discuss them because the ²⁷Al concentrations may have been underestimated for at least several samples, so the ²⁶Al exposure ages are not included in the moraine age calculation here.

³To calculate this moraine age and statistics, we: include the oldest boulder on the Roanoke Point moraine (LI-8); exclude the youngest four boulders on the Buzzards Bay moraine, as well as sample GB2002-BB2-29-1 because including it raises the reduced χ^2 value to ~ 40 ; and exclude the youngest boulder on the Charlestown moraine. Including sample GB2002-BB2-29-1 in the average does not change the rounded exposure age reported here.

⁴Sample GB2002-BB2-29-1 is excluded from the average because including it raises the reduced χ^2 value to ~ 40 . Including this sample does not affect the rounded exposure age reported here.

490 rock. If some boulders were sourced above this zone (~2–6 m), we would expect to see more scatter in these exposure-
 491 age datasets; if at least some boulders were sourced below these depths, inherited muon-produced ¹⁰Be in those
 492 samples would be negligible, but together with boulders sourced from above or within this zone, the age distribution
 493 would still skew old (Briner et al., 2016b). The morphology of the moraines along with the uniform age distributions
 494 and lack of scatter suggest that the exposure ages on these moraines represent their true deposition age within
 495 uncertainties (Table 2).
 496

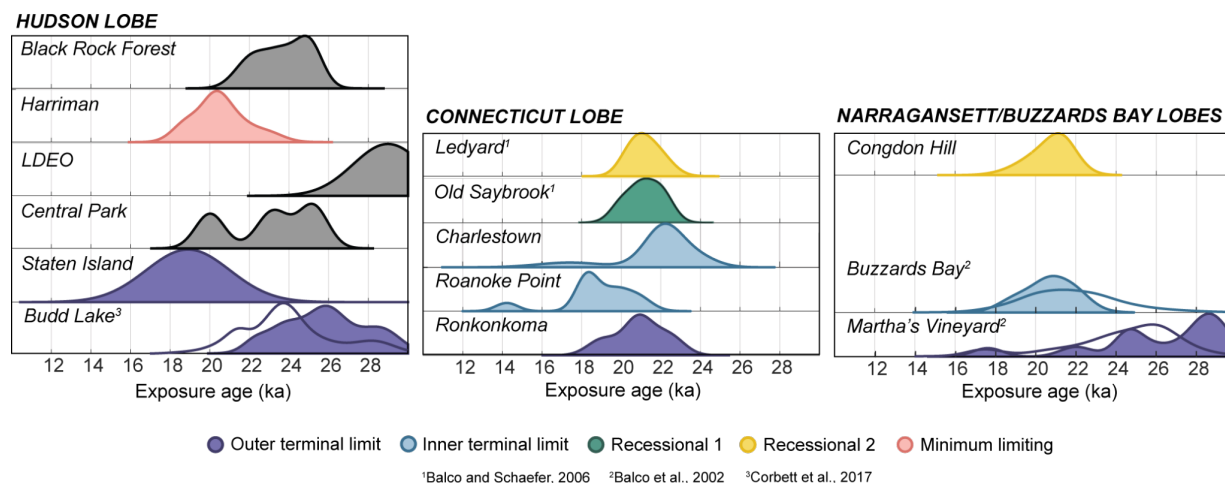
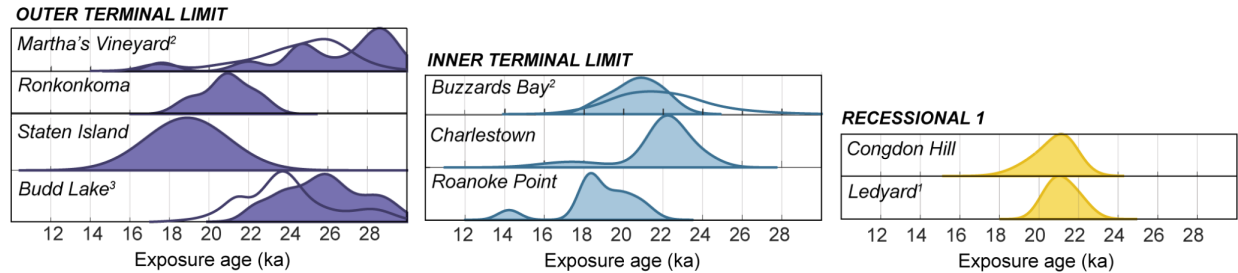


Figure 6 - Camel plots for moraine exposure ages grouped by LIS lobe. Colors are the same as Figure 1. Filled camel plots show the relative probability distribution for the ¹⁰Be age of the moraine and open camel plots show the probability distribution for the ²⁶Al age. Note the normal age distributions of the Ledyard, Old Saybrook, Charlestown and Harriman moraine boulders compared to the age distribution of the Martha’s Vineyard moraine, which likely includes both postdepositional disturbance (young outliers) and inheritance (old outliers). See Tables 1 and S2 for outlier identification.

497
 498 Instead, the preponderance of boulders with ages that may be slightly younger than the true emplacement age
 499 on the Ronkonkoma, Roanoke Point and Buzzards Bay moraines is most likely explained by a small degree of
 500 postdepositional disturbance. These large end moraines have broad, relatively flat crests comprising a complex of
 501 moraine ridges with kettle and kame topography, indicating that the moraines were almost certainly ice cored after
 502 the LIS abandoned these positions and underwent post-emplacement settling. In addition, agricultural disturbances or
 503 other human-induced environmental modification may have contributed to the movement or exhumation of boulders
 504 on these moraines. Balco (2011) recognized that the Buzzards Bay ¹⁰Be and ²⁶Al measurements, independent analyses
 505 that should be uncorrelated if scatter in the dataset is due to measurement error alone, were in fact correlated unless
 506 the four youngest ages are discarded, indicating the presence of geologic scatter. A moderate relationship between
 507 boulder height and exposure age ($r^2 = 0.36$) suggests that sediment or snow cover is a likely source of this scatter
 508 (Balco, 2011). Discarding the four youngest ages gives an average age of 22.1 ± 0.6 ka for the Buzzard’s Bay moraine.
 509 The geomorphic setting of the boulders sampled on the Ronkonkoma and Roanoke Point moraines indicates a similar
 510 role for post depositional disturbance as on the Buzzards Bay moraine. Boulders suitable for exposure-age dating were

511 difficult to locate on the Ronkonkoma moraine as the moraine comprises mostly sandy outwash till, which may have
 512 been affected by LIS meltwater as it occupied a more northern position (Section 2.1.1). Samples on the Roanoke Point
 513 moraine generally came from large boulders (>1 m) situated in local depressions and/or inboard of the moraine crest
 514 (Section 2.1.1; Figure S1), so may have been



¹Balco and Schaefer, 2006 ²Balco et al., 2002 ³Corbett et al., 2017

Figure 7 - Camel plots for moraine exposure ages grouped by ice-margin limit. Colors are the same as Figure 1 and only ice-margin limits with more than one moraine are shown. Filled camel plots show the probability distribution for the ¹⁰Be age of the moraine and open camel plots show the probability distribution for the ²⁶Al age.

515 subjected to hillslope processes and/or been encased in stagnant ice even after initial moraine abandonment. It is also
 516 possible these boulders were affected by human modification of the environment. In contrast, the two oldest boulders
 517 on the Roanoke Point moraine (LI-1, 20.1 ± 1.0 ka and LI-8, 20.9 ± 0.7 ka), while also located slightly inboard of the
 518 moraine crest, rest on local highs where they may have been more stable (Figure S1).

519 Given the geomorphic context of the Ronkonkoma, Roanoke Point and Buzzards Bay samples, it is possible
 520 that averaging the exposure ages of all boulders from these moraines slightly underestimates the true emplacement
 521 age. On the other hand, the oldest exposure ages from the Ronkonkoma, Roanoke Point and Buzzards Bay moraines
 522 generally overlap with the age distributions of stratigraphically equivalent or inboard moraines (Figures 6 and 7),
 523 suggesting that the oldest ages of the main population are a better estimate of the emplacement age than the average
 524 age. The wide age distribution on the Martha's Vineyard moraine, which includes young ages (~17 ka), is also
 525 consistent with the interpretation that at least parts of the large, hummocky end moraines are affected by
 526 postdepositional disturbance (Figures 6 and 7; Balco et al., 2002). The Martha's Vineyard age distribution also
 527 includes older ages indicative of inheritance, which is to be expected given that the first advance of the LIS to its
 528 terminal position likely remobilized boulders exposed during the preceding interglacial period and prior to expansion
 529 to the southernmost limits.

530 Guided by these arguments, we present emplacement ages for the moraines deposited by the Connecticut and
 531 Narragansett-Buzzards Bay Lobes of the LIS, recognizing that they are differentially affected by postdepositional
 532 disturbance and nuclide inheritance. For the Martha's Vineyard moraine, we take the average of the ¹⁰Be and ²⁶Al
 533 ages of the main population, which yields an age of 25.4 ± 2.5 ka (Balco et al., 2002). The oldest age on the
 534 Ronkonkoma moraine (22.4 ± 0.8 ka) is probably closer to the true deposition age than the average (20.8 ± 1.4 ka),
 535 although they do overlap within uncertainty. For the Roanoke Point-Charlestown-Buzzards Bay limit, we take the
 536 average age of the Buzzards Bay boulders, excluding the four youngest (Balco, 2011); the oldest boulder on Roanoke

537 Point moraine; and the main age population on Charlestown moraine, which gives an age for this limit of 22.2 ± 0.8
538 ka (Table 2). We take the average age of the Old Saybrook moraine to represent its true deposition age (21.1 ± 0.8 ka;
539 Balco and Schaefer, 2006). The Ledyard Moraine (Balco and Schaefer, 2006) and Congdon Hill moraines are
540 stratigraphically correlated, and their exposure ages agree within measurement uncertainty (reduced X^2 of combined
541 population = 1), so we combine their exposure ages to represent the true age of the limit (21.0 ± 0.8 ka; Table 2).

542

543 **5.1.2 Hudson Lobe**

544 The exposure-age, radiocarbon, and OSL chronologies for LIS retreat in the Hudson River Valley are
545 generally consistent, although some conflicts remain (Figures 2 and 3). As described in detail in previous studies, the
546 cosmogenic exposure ages at the Budd Lake moraine (25.7 ± 2.0 ka; Corbett et al., 2017) agree within uncertainty
547 with the maximum-limiting radiocarbon ages in Long Island and in Manhattan (26.1–25.8 ka; Schuldenrein and
548 Aiuvalasit, 2011; Sirkin and Stuckenrath, 1980), maximum-limiting OSL ages at Jones Point, New York (25.3 ± 7.4
549 ka; Gorokhovich et al., 2018), and a minimum-limiting radiocarbon age of 24.2 ± 1.1 ka in a concretion of postglacial
550 lake sediment just south of the terminal moraine (Stanford et al., 2021). The Budd Lake moraine exposure ages also
551 overlap with the age distribution on the Martha’s Vineyard moraine (Section 5.1.1; Balco et al., 2002; Corbett et al.,
552 2017). Two boulders on the Harbor Hill moraine on Staten Island, New York, have disparate ages (18.9 ka and 41.6
553 ka; Table 1), similar to the distribution of ages on Martha’s Vineyard, which is affected by inheritance and
554 postdepositional disturbance (Figure S3). Therefore, we cannot disprove the hypothesis that the moraine on Staten
555 Island was deposited at the same time as the Budd Lake, Ronkonkoma, and Martha’s Vineyard moraines, as the
556 stratigraphic correlation suggests.

557 Exposure ages on bedrock surfaces in New York City and the lower Hudson Valley are consistently older
558 than co-located boulders. Two bedrock ages (25.0 ± 0.7 and 23.2 ± 0.8 ka) in Central Park, New York are older than
559 a nearby boulder (20.0 ± 0.7 ka); a single bedrock sample at the Lamont-Doherty Earth Observatory dates to $29.0 \pm$
560 1.8 ka; and at Black Rock Forest three bedrock ages (one of 25.0 ± 0.7 ka and two of $\sim 100 \pm 3$ ka) are significantly
561 older than two boulder samples from the same location (22.1 ± 0.8 ka and 23.7 ± 0.8 ka; Figure 3). Furthermore, the
562 bedrock ages at LDEO and Black Rock Forest are older than nearby radiocarbon ages that suggest the ice margin did
563 not retreat north of LDEO until ~ 22.5 ka and north of Black Rock Forest until ~ 20 – 19 ka (Stanford et al., 2021). The
564 fact that bedrock exposure ages significantly pre-date nearby boulders and radiocarbon ages indicates cosmogenic-
565 nuclide inheritance, implying that erosion beneath the LIS at these sampling locations was insufficient to remove ^{10}Be
566 to background levels in bedrock, perhaps because ice was thin and slow-flowing or because of short ice-cover
567 durations, or both. The three erratic boulder ages in our Hudson Valley transect do not exhibit a clear trend with
568 distance from the terminal moraine, where the age in Central Park (20.0 ka) is significantly younger than two ages at
569 Black Rock Forest (22.1 ka and 23.7 ka), ~ 80 km to the north. Given the presence of inheritance in the bedrock ages
570 and lack of spatial trend in the boulder ages in the Hudson Valley, we exclude these ages from further discussion here,
571 and identify additional collection of bedrock and boulder samples in this region as a potential direction for future
572 work.

573 The average age of the ice-marginal deposit in Harriman State Park (20.4 ± 1.3 ka; Figures 3 and 6) is
574 consistent with the minimum-limiting age of the varve sequence at Haverstraw, New York (18.9 ka; Ridge et al.,
575 2012), situated a similar distance from the terminal moraine, and is older than the youngest boulder age on a former
576 nunatak at Peekamoose Mountain (18.6 ka) ~80 km to the north (Halsted et al., 2022). Finally, the average ^{10}Be age
577 of the Harriman State Park boulders of 20.4 ± 1.3 ka is slightly younger than the Ledyard moraine exposure age (21.2
578 ± 0.7 ka), although the ages overlap within 1σ uncertainty, supporting the correlation of the Augusta and Sussex limits
579 in northern New Jersey with the Connecticut moraines (Section 1.1.1; Stone et al., 2005). This interpretation, however,
580 remains in disagreement with recent work that suggests all three moraines in northern New Jersey are ~23.5, and that
581 the Connecticut moraines may instead correlate with the Pellets Island and New Hampton moraines to the north
582 (Figure 1; Stanford et al., 2021). Nevertheless, the age of the Harriman State Park ice-marginal deposit agrees with
583 the majority of bulk radiocarbon ages in northern New Jersey as summarized by Stanford et al. (2021; Figure 2).

584

585 **5.1.3 Summary of regional deglaciation chronology**

586 To summarize the exposure-age chronology, the southeastern LIS occupied the terminal complex from ~26
587 to 22 ka, with the outermost moraine ridges dating to 25.4 ± 2.5 ka at Martha's Vineyard (Balco et al., 2002) and 25.7
588 ± 2.0 ka at Budd Lake in New Jersey (Corbett et al., 2017). The inner terminal limit at Roanoke Point-Charlestown-
589 Buzzards Bay, located 10–30 km north of the outer terminal ridge, dates to 22.2 ± 0.8 ka. The fact that the innermost
590 portion of the terminal complex is nearly 4 kyr younger than the outermost ridges could represent slow, secular retreat
591 of the ice margin through this period, or the position of the moraines could reflect fluctuations of the ice margin during
592 the LGM, with the culmination of readvances occurring within the terminal moraine belt. We prefer the latter
593 interpretation given that the geomorphology and sedimentology of these moraines indicate construction by an
594 advancing LIS and note that it is unknown how far ice retreated between readvances (Boothroyd et al., 1998; Oldale
595 and O'Hara, 1984; Sections 1.1.1 and 2.2.1).

596 Irreversible deglaciation began with the abandonment of the inner terminal moraine at ~22 ka, after which
597 the ice margin did not reoccupy the terminal complex. Ice-margin positions in southern Connecticut and Rhode Island
598 are marked by smaller, discontinuous, boulder-rich moraines interpreted as recessional limits deposited during brief
599 re-advances or standstills (Stone et al., 2005). The Old Saybrook moraine, ~40 km inboard of the outer terminal limit,
600 is 21.1 ± 0.8 ka (Balco and Schaefer, 2006), and the Ledyard-Congdon Hill limit ~45–50 km north of the outer terminal
601 ridge, is 21.0 ± 0.8 ka. The ice-marginal deposit in Harriman State Park, which is morpho-stratigraphically inboard of
602 the Ledyard-Congdon Hill limit, is 20.4 ± 1.3 ka. Therefore, the exposure-age chronology presented here spans ~25.5–
603 20.5 ka. The LIS then retreated to the spillway for glacial Lake Hitchcock in Rocky Hill, CT, ~90–100 km north of
604 the outer terminal moraine, by ~18.2 ka (Ridge et al., 2012). A lack of extensive end moraine deposits between the
605 Ledyard-Congdon Hill limit and Rocky Hill, CT signals a shift to more continuous retreat north of our study area.

606 The positions of the moraines represent net changes in LIS extent from which we estimate average retreat
607 rates, calculated using the maximum and minimum distance between moraine ridges measured parallel to the transect
608 in Figure 1, divided by the difference in age established for each limit (Table 2; Figure 8). Although these rates
609 represent overall northward movement of the ice-margin position (i.e., retreat), they integrate periods of retreat,

610 advance, and minimal change given that the moraines themselves were formed during readvances or standstills. In
611 this context, the terminal moraine belt represents several ice-margin fluctuations, with the rate of change in ice-margin
612 position from the outer terminal to inner terminal limit averaging $<5\text{--}10\text{ m yr}^{-1}$. Ice then retreated from the inner
613 terminal position to the Ledyard-Congdon Hill limit at an average rate of $\sim 10\text{--}20\text{ m yr}^{-1}$. Further retreat through
614 southern Connecticut and Rhode Island was interrupted by several standstills or re-advances during which additional
615 recessional moraines, including the Old Saybrook moraine, were deposited. After abandoning of the Old Saybrook
616 moraine, the LIS withdrew to Rocky Hill, Connecticut, at an average rate of $\sim 15\text{--}25\text{ m yr}^{-1}$ (Ridge et al., 2012). North
617 of our study area, the NAVC reveals moderate retreat rates of $\sim 30\text{--}100\text{ m yr}^{-1}$ during Heinrich Stadial 1 ($\sim 18\text{--}15\text{ ka}$),
618 with an abrupt increase in retreat rate to $>300\text{ m yr}^{-1}$ at the onset of the Bølling-Allerød $\sim 15\text{ ka}$ (Figure 8; Ridge et al.,
619 2012). A prominent set of moraines along coastal Maine also may suggest slow but steady net retreat during the latter
620 part of Heinrich Stadial 1 (Borns et al., 2004; Kaplan, 1999; Hall et al., 2017). Similar retreat rates ($100\text{--}300\text{ m yr}^{-1}$)
621 are implied by DeGeer moraines interpreted to mark the annual retreat of the ice margin in southern New Hampshire,
622 Maine and Atlantic Canada around 15 ka (Sinclair et al., 2018; Todd et al., 2007; Wroblewski, 2020). Cosmogenic-
623 exposure ages from former nunataks that serve as “dipsticks” for LIS thickness also show moderate thinning through
624 HS1 followed by rapid LIS thinning at the onset of the Bølling (Halsted et al., 2022).

625 The regional moraine chronology is remarkably consistent with the varve chronologies, OSL ages, and many
626 of the radiocarbon ages throughout the region, as discussed above (Figure 5). Yet, the absence of radiocarbon ages on
627 plant macrofossils between ~ 26 and 16 ka remains unresolved (Peteet et al., 2012; Figures 2, 3, and 5). This absence
628 could potentially be explained by i) poor preservation of macrofossils from this time period, ii) landscape instability
629 and/or sparse vegetation in the study area during the LGM and early deglaciation, iii) the delay of widespread organic
630 sediment deposition until beaver colonies expanded into the region, damming lakes and wetlands (Kaye, 1962), iv)
631 the predominance of seepage ponds in permeable sand and other ice proximal coarse deposits on end moraines which
632 are susceptible to periodic drainage, v) difficulty in coring to the till contact and/or stratigraphic disturbance in lake
633 sediment affected by postglacial permafrost (Prince et al., 2024) and/or vi) persistent lake ice during HS1 ($\sim 18\text{--}15\text{ ka}$)
634 spring or summers that precluded organic lake sedimentation. Further discussion of the $\sim 10\text{ kyr}$ gap between the
635 moraine emplacement age indicated by the exposure-age chronology and the widespread occurrence of radiocarbon-
636 dated organic material 16 ka is beyond the scope of this paper.

637

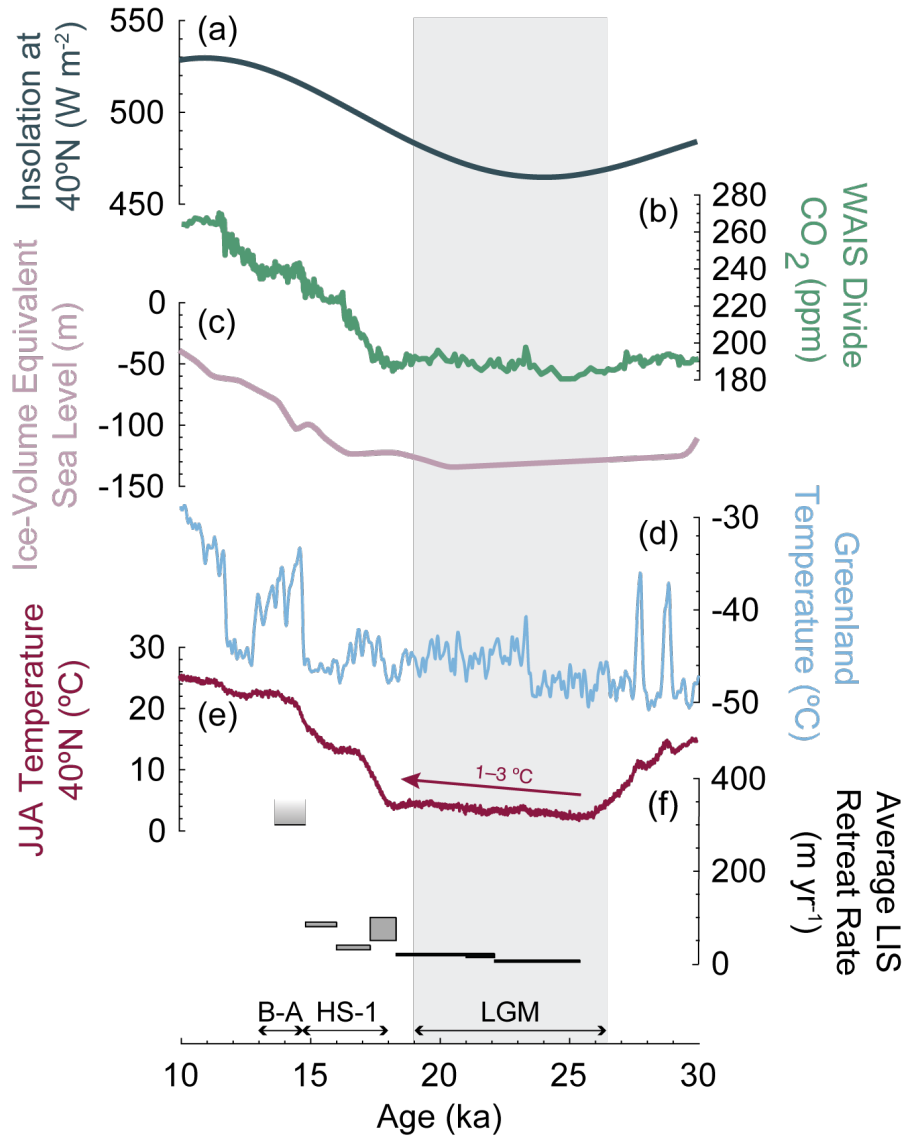


Figure 8 - LIS ice-margin chronology and average retreat rates compared to other climate parameters and records. a) June 21st insolation at 40°N (Laskar et al., 2004). b) compilation of atmospheric CO₂ measured in Antarctic ice cores (Bereiter et al., 2014; Monnin et al., 2001, 2004; Marcott et al., 2014; Ahn et al., 2014). c) global ice-volume equivalent sea-level (Lambeck et al., 2014). d) Greenland mean-annual temperature reconstruction based on $\delta^{15}\text{N}-\text{N}_2$ in the NGRIP ice core (Kindler et al., 2014). e) time series of summer (June, July and August) surface temperatures modeled using the Had3CMB-M2.1 coupled general circulation model that incorporates Dansgaard-Oeschger and Heinrich events (Armstrong et al., 2019). The time series shown here is for 40°N, 75.5°W, ~50 km south of the LGM limit in a part of northern New Jersey that was not covered by ice during the LGM. f) Average LIS retreat rates. Rates shown in black are from this study and those shown in gray are from Ridge et al. (2012), with the faded gray bar indicating a minimum retreat rate of 300 m yr⁻¹. The range of average retreat rates are calculated using the maximum and minimum distance between moraine ridges measured parallel to the transect in Figure 1, divided by the difference in age established for each limit (Table 2). Vertical gray bar in the background denotes the LGM timing from 26.5–19 ka (Clark et al., 2009). Heinrich Stadial 1 (HS-1; ~18–15 ka) and Bølling-Allerød (B-A; ~15–13 ka) are periods of abrupt climate change discussed in the text.

639 5.2 Climatic context for initial LIS retreat

640 The exposure-age-derived moraine chronology suggests that the LIS occupied the terminal moraine complex
641 between ~26 and 22 ka and remained within 50 km of its southernmost position until ~21 ka (Balco et al., 2002; Balco
642 and Schaefer, 2006; Corbett et al., 2017). The moraines discussed here therefore span the canonical LGM and global
643 sea-level lowstand (26.5–19.0 ka; Lambeck et al., 2014; Clarke et al., 2009) and coincide with a local insolation
644 minimum at ~24 ka (Figure 8; Laskar et al., 2004). Furthermore, the timing of terminal moraine occupation from ~26
645 to 22 ka is similar to that of other LIS sectors to the west, as well as other ice sheets fringing the North Atlantic (Balco
646 et al., 2002; Corbett et al., 2017; Section 5.1.3). For example, exposure and radiocarbon ages indicate the glacial
647 maximum occurred in Wisconsin and Illinois by ~24–23 ka (Ullman et al., 2015; Currey and Petras, 2011) and a
648 minimum limiting radiocarbon age on the terminal moraine of the Miami-Scioto lobe in Indiana and Ohio indicates
649 retreat began sometime before 22.4 ka (Glover et al., 2011). Parts of the British-Irish Ice Sheet began to retreat by
650 ~30–26 ka (Clark et al., 2022) and the Scandinavian ice sheet on Andøya, Norway, fluctuated near its maximum extent
651 from ~26–22 ka (Vorren et al., 2015). Retreat from the terminal moraine complex ~22 ka is consistent with ice-sheet
652 mass balance modeling, which indicates that the moderate increase in local summer insolation beginning ~24 ka may
653 have driven initial LIS margin retreat from its southernmost position (Ullman et al., 2015). We emphasize, however,
654 that the ~50 km of net change in ice-margin position from the outer terminal moraine to the Ledyard-Congdon Hill
655 limit is modest in the context of the entire ice sheet. This distance represents <2% of total LIS margin change
656 considering that the former LIS is now restricted to the Barnes and Penny Ice Caps on the central Baffin plateau ~3000
657 km to the north (Dalton et al., 2020; Dyke, 2004; Hooke, 1976; Hooke and Clausen, 1982; Refsnider et al., 2014), and
658 likely significantly less when expressed volumetrically since the LIS would have been thinner at its margin than
659 towards the centre of the ice sheet (e.g., Stokes et al., 2012).

660 The chronology supports the hypothesis that initial LIS retreat, albeit slow (<5–25 m yr⁻¹; Section 5.1.3),
661 began when cold mean-annual temperatures persisted in the Arctic (Kindler et al., 2014) and atmospheric CO₂
662 concentrations remained at glacial values (Figure 8; Denton et al., 2010; Marcott et al., 2014; Raymo, 1997; Ullman
663 et al., 2015; Figure 8). Yet, insight into local summer conditions may provide additional context for the relatively
664 modest LIS retreat during the LGM. Ridge et al. (2012) established a strong relationship, especially after ~15 ka,
665 between LIS retreat rates, the Greenland temperature record, and local summer conditions as recorded by varve
666 thickness, which is largely controlled by LIS meltwater production. In the absence of varve thickness as a proxy for
667 summer climate conditions prior to ~18 ka, we use output from a recent model reconstruction of Northern Hemisphere
668 land surface air temperatures over the last 60 kyr to estimate changes in summer temperature coincident with the
669 moraine chronology discussed here (Figure 8; Armstrong et al., 2019). Modeled terrestrial summer temperature at
670 40°N, 75.5°W, ~50 km south of the LGM limit in northern New Jersey, exhibits a slow but steady increase of ~1–3°C
671 from 26–19 ka and sharp rise beginning at ~18 ka (Figure 8; Armstrong et al., 2019). The pattern of modeled summer
672 temperature change bears striking resemblance to the slow net LIS retreat (<5–25 m yr⁻¹) from ~26–21 ka as indicated
673 by the moraine record, and acceleration of ice-margin retreat after ~18 ka (30–>300 m yr⁻¹), as observed in the NAVC
674 (Ridge et al., 2012). We therefore suggest that the relationship between LIS behavior, including relative ice margin

675 positions, and summer conditions observed by Ridge et al. (2012) extends to the LGM. Altogether, the moraine record
676 in southern New England and New York records LIS fluctuations and modest retreat through the LGM, consistent
677 with a slight increase in modeled summer temperature during that interval, with deglaciation accelerating after 18 ka
678 alongside the rise in atmospheric CO₂ and the onset of Termination 1.

679 **6 Conclusions**

- 680 ● The exposure-age chronology in southern New England and New York agrees with established regional
681 stratigraphic relationships and independent age constraints from radiocarbon and glacial lake varves.
- 682 ● The few inconsistencies in the regional exposure-age dataset can be explained by systematic geologic scatter
683 where i) bedrock samples are affected by nuclide inheritance, ii) the outermost LGM moraine exhibits
684 inheritance on some boulders, and iii) some exposure ages on large unconsolidated landforms that may have
685 experienced extended permafrost conditions are affected by postdepositional disturbance while more stable
686 landforms are not. Also, we cannot rule out that the boulders with the youngest exposure were affected by
687 agricultural practices and other human activities.
- 688 ● Considering the impact of this geologic scatter, we conclude that the LIS occupied the terminal complex from
689 ~26 ka to ~22 ka (Balco, 2011; Balco et al., 2002). We date several inboard moraines and other recessional
690 deposits to ~21–20.5 ka (Balco and Schaefer, 2006).
- 691 ● The moraine chronology for the southeastern LIS spans ~26–21 ka, which is consistent with the canonical
692 LGM and sea-level lowstand, full glacial conditions in Greenland, and is broadly coincident with a minimum
693 in local summer insolation.
- 694 ● Average LIS retreat rates from ~26–18 ka (<5 to 25 m yr⁻¹) are consistent with slight warming (1–3°C) in
695 modeled local summer temperature through the LGM, but were slower than at any point during Termination
696 1 (>30 to >300 m yr⁻¹; Ridge et al., 2012), although this does not account for any distance covered by the
697 readvance or stillstand, if significant. Hence, we conclude that the major pulse of deglaciation and marked
698 recession did not begin until after ~18 ka, when a dramatic rise in atmospheric CO₂ signals the onset of
699 Termination 1.

700

701 **Data Availability**

702 All analytical information associated with new cosmogenic-nuclide measurements appear in the tables and
703 Supplement. Analytical information, with additional sample documentation and photographs, is also available in the
704 ICED:LAURENTIDE online database (<https://version2.ice-d.org/laurentide/publication/1187/>, Balco, 2024).
705

706 **Competing Interests**

707 The contact author has declared that none of the authors has any competing interests.

708 **Acknowledgements**

709 We thank the many people who helped support this work in the lab and field, including Sidney Hemming, as well as
710 Mikah McCabe and Rebecca Steinberg who helped collect and process samples as interns in the Lamont-Doherty
711 Earth Observatory Summer Intern Program. We are immensely grateful to the late Jon Boothroyd of the University
712 of Rhode Island and the late Gil Hanson of Stony Brook University for sharing their expertise in the regional
713 stratigraphy and geomorphology. This work was supported in part by the National Science Foundation Graduate
714 Research Fellowship under grant no. DGE 2036197 to Allie Balter-Kennedy. Joerg Schaefer acknowledges support
715 by the Vetlesen Foundation and the LDEO Climate Center.

716 **References**

- 717 Andersen, K. K., Svensson, A., Johnsen, S. J., Rasmussen, S. O., Bigler, M., Röthlisberger, R., Ruth, U., Siggaard-
718 Andersen, M.-L., Steffensen, J. P., Dahl-Jensen, D., Vinther, B. M., and Clausen, H. B.: The Greenland Ice
719 Core Chronology 2005, 15–42ka. Part 1: constructing the time scale, *Quaternary Sci Rev*, 25, 3246–3257,
720 <https://doi.org/10.1016/j.quascirev.2006.08.002>, 2006.
- 721 Antevs, E.: The last glaciation, with special reference to the ice sheet in northeastern North America, *American*
722 *Geographical Society Research Series*, 292, 1928.
- 723 Antevs, E.: The recession of the last ice sheet in New England. *American Geographical Society Research Series* 11
724 (with a preface and contributions by J. W. Goldthwait) 120, 1922.
- 725 Applegate, P. J., Urban, N. M., Keller, K., Lowell, T. V., Laabs, B. J. C., Kelly, M. A., and Alley, R. B.: Improved
726 moraine age interpretations through explicit matching of geomorphic process models to cosmogenic nuclide
727 measurements from single landforms, *Quaternary Res*, 77, 293–304,
728 <https://doi.org/10.1016/j.yqres.2011.12.002>, 2012.
- 729 Applegate, P. J., Urban, N. M., Laabs, B. J. C., Keller, K., and Alley, R. B.: Modeling the statistical distributions of
730 cosmogenic exposure dates from moraines, *Geosci Model Dev*, 3, 293–307, [https://doi.org/10.5194/gmd-3-](https://doi.org/10.5194/gmd-3-293-2010)
731 293-2010, 2010.
- 732 Armstrong, E., Hopcroft, P. O., and Valdes, P. J.: A simulated Northern Hemisphere terrestrial climate dataset for the
733 past 60,000 years, *Sci Data*, 6, 265, <https://doi.org/10.1038/s41597-019-0277-1>, 2019.
- 734 Balco, G. and Schaefer, J. M.: Cosmogenic-nuclide and varve chronologies for the deglaciation of southern New
735 England, *Quat Geochronol*, 1, 15–28, <https://doi.org/10.1016/j.quageo.2006.06.014>, 2006.
- 736 Balco, G., Briner, J., Finkel, R. C., Rayburn, J. A., Ridge, J. C., and Schaefer, J. M.: Regional beryllium-10 production
737 rate calibration for late-glacial northeastern North America, *Quat Geochronol*, 4, 93–107,
738 <https://doi.org/10.1016/j.quageo.2008.09.001>, 2009.
- 739 Balco, G., DeJong, B. D., Ridge, J. C., Bierman, P. R., and Rood, D. H.: Atmospherically produced beryllium-10 in
740 annually laminated late-glacial sediments of the North American Varve Chronology, *Geochronology*, 3, 1–
741 33, <https://doi.org/10.5194/gchron-3-1-2021>, 2021.
- 742 Balco, G., Stone, J. O. H., Porter, S. C., and Caffee, M. W.: Cosmogenic-nuclide ages for New England coastal
743 moraines, Martha’s Vineyard and Cape Cod, Massachusetts, USA, *Quaternary Sci Rev*, 21, 2127–2135,
744 [https://doi.org/10.1016/s0277-3791\(02\)00085-9](https://doi.org/10.1016/s0277-3791(02)00085-9), 2002.
- 745 Balco, G., Stone, J. O., Lifton, N. A., and Dunai, T. J.: A complete and easily accessible means of calculating surface
746 exposure ages or erosion rates from ^{10}Be and ^{26}Al measurements, *Quat Geochronol*, 3, 174–195,
747 <https://doi.org/10.1016/j.quageo.2007.12.001>, 2008.
- 748 Balco, G.: Contributions and unrealized potential contributions of cosmogenic-nuclide exposure dating to glacier
749 chronology, 1990–2010, *Quaternary Sci Rev*, 30, 3–27, <https://doi.org/10.1016/j.quascirev.2010.11.003>,
750 2011.

751 Balco, G.: ICE-D:LAURENTIDE, available at: <https://version2.ice-d.org/laurentide/publication/1187/>, last access: 11
752 July 2024.

753 Balco, G.: Production rate calculations for cosmic-ray-muon-produced ¹⁰Be and ²⁶Al benchmarked against
754 geological calibration data, *Quat. Geochronol.*, 39, 150–173, <https://doi.org/10.1016/j.quageo.2017.02.001>,
755 2017.

756 Barker, S. and Knorr, G.: Millennial scale feedbacks determine the shape and rapidity of glacial termination, *Nat*
757 *Commun*, 12, 2273, <https://doi.org/10.1038/s41467-021-22388-6>, 2021.

758 Barker, S., Diz, P., Vautravers, M. J., Pike, J., Knorr, G., Hall, I. R., and Broecker, W. S.: Interhemispheric Atlantic
759 seesaw response during the last deglaciation, *Nature*, 457, 1097–1102, <https://doi.org/10.1038/nature07770>,
760 2009.

761 Boothroyd, J. C., and Sirkin, L.: The Quaternary geology of Block Island and adjacent regions, in Paton, P., Gould,
762 L. I., August, P. V., and Frost, A. O., eds., *The Ecology of Block Island: Kingston, Rhode Island*, Rhode
763 Island Natural History Survey, p. 13-27, 2002.

764 Boothroyd, J. C., McCandless, S. J., and Dowling, M. J.: Quaternary Geologic Map of Rhode Island: Rhode Island
765 Geological Survey STATEMAP Program, scale scale: 1:100,000.
766 http://geothermal.igs.illinois.edu/aasggeothermal/rigs/map/RI_Quaternary_Geology_100K.zip, 2003.

767 Boothroyd, J.C., Freedman, J.H., Brenner, H.B., Stone, J.R.: The Glacial Geology of Southern and Central Rhode
768 Island, in: Murray, D.P. (Ed.), *Guidebook to Field Trips in Rhode Island and Adjacent Regions of*
769 *Connecticut and Massachusetts*. Presented at the New England Intercollegiate Geological Conference: 90th
770 Annual Meeting, Kingston, Rhode Island, pp. C5-1:25., 1998.

771 Borchers, B., Marrero, S., Balco, G., Caffee, M., Goehring, B., Lifton, N., Nishiizumi, K., Phillips, F., Schaefer, J.,
772 and Stone, J.: Geological calibration of spallation production rates in the CRONUS-Earth project, *Quat*
773 *Geochronol*, 31, 188–198, <https://doi.org/10.1016/j.quageo.2015.01.009>, 2016.

774 Borns, H. W., Doner, L. A., Dorion, C. C., Jacobson, G. L., Kaplan, M. R., Kreutz, K. J., Lowell, T. V., Thompson,
775 W. B., and Weddle, T. K.: The deglaciation of Maine, U.S.A., *Dev. Quat. Sci.*, 2, 89–109,
776 [https://doi.org/10.1016/s1571-0866\(04\)80190-8](https://doi.org/10.1016/s1571-0866(04)80190-8), 2004.

777 Briner, J. P., Goehring, B. M., Mangerud, J., and Svendsen, J. I.: The deep accumulation of ¹⁰Be at Utsira,
778 southwestern Norway: Implications for cosmogenic nuclide exposure dating in peripheral ice sheet
779 landscapes, *Geophys Res Lett*, 43, 9121–9129, <https://doi.org/10.1002/2016gl070100>, 2016.

780 Briner, J. P., McKay, N. P., Axford, Y., Bennike, O., Bradley, R. S., Vernal, A. de, Fisher, D., Francus, P., Fréchette,
781 B., Gajewski, K., Jennings, A., Kaufman, D. S., Miller, G., Rouston, C., and Wagner, B.: Holocene climate
782 change in Arctic Canada and Greenland, *Quaternary Sci Rev*, 147, 340–364,
783 <https://doi.org/10.1016/j.quascirev.2016.02.010>, 2016.

784 Brock, P. C. and Brock, P. W. G.: Bedrock Geology of New York City: More than 600 m.y. of geologic history" Field
785 Guide for Long Island Geologists Field Trip, October 27, 2001, in: *Field Guide for Long Island Geologists*
786 *Field Trip*, 2001.

787 Broecker, W. S. and Donk, J., van: Insolation changes, ice volumes, and the O18 record in deep-sea cores, *Rev*
788 *Geophys*, 8, 169–198, <https://doi.org/10.1029/rg008i001p00169>, 1970.

789 Bromley, G. R. M., Hall, B. L., Thompson, W. B., and Lowell, T. V.: Age of the Berlin moraine complex, New
790 Hampshire, USA, and implications for ice sheet dynamics and climate during Termination 1, *Quaternary*
791 *Res*, 94, 80–93, <https://doi.org/10.1017/qua.2019.66>, 2020.

792 Buizert, C., Gkinis, V., Severinghaus, J. P., He, F., Lecavalier, B. S., Kindler, P., Leuenberger, M., Carlson, A. E.,
793 Vinther, B., Masson-Delmotte, V., White, J. W. C., Liu, Z., Otto-Bliesner, B., and Brook, E. J.: Greenland
794 temperature response to climate forcing during the last deglaciation, *Science*, 345, 1177–1180,
795 <https://doi.org/10.1126/science.1254961>, 2014.

796 Cadwell, D.H.: *Surficial Geologic Map of New York: Lower Hudson Sheet*. New York State Museum Map and Chart
797 Series. The University of the State of New York, Albany, NY, 1989.

798 Clark, P. U., Dyke, A. S., Shakun, J. D., Carlson, A. E., Clark, J., Wohlfarth, B., Mitrovica, J. X., Hostetler, S. W.,

799 and McCabe, A. M.: The Last Glacial Maximum, *Science*, 325, 710–714,
800 <https://doi.org/10.1126/science.1172873>, 2009.

801 Clark, P. U., Licciardi, J. M., MacAyeal, D. R., and Jenson, J. W.: Numerical reconstruction of a soft-bedded
802 Laurentide Ice Sheet during the last glacial maximum, *Geology*, 24, 679–682, 1996.

803 Clark, P. U., Marshall, S. J., Clarke, G. K. C., Hostetler, S. W., Licciardi, J. M., and Teller, J. T.: Freshwater Forcing
804 of Abrupt Climate Change During the Last Glaciation, *Science*, 293, 283–287,
805 <https://doi.org/10.1126/science.1062517>, 2001.

806 Collins, G.: The Very Cold Case of the Glacier. *The New York Times*, 2005.

807 Corbett, L. B., Bierman, P. R., Stone, B. D., Caffee, M. W., and Larsen, P. L.: Cosmogenic nuclide age estimate for
808 Laurentide Ice Sheet recession from the terminal moraine, New Jersey, USA, and constraints on latest
809 Pleistocene ice sheet history, *Quaternary Res*, 87, 482–498, <https://doi.org/10.1017/qua.2017.11>, 2017.

810 Crump, S. E., Anderson, L. S., Miller, G. H., and Anderson, R. S.: Interpreting exposure ages from ice-cored moraines:
811 a Neoglacial case study on Baffin Island, Arctic Canada, *J. Quaternary Sci.*, 32, 1049–1062,
812 <https://doi.org/10.1002/jqs.2979>, 2017.

813 Cuffey, K. M., Clow, G. D., Steig, E. J., Buizert, C., Fudge, T. J., Koutnik, M., Waddington, E. D., Alley, R. B., and
814 Severinghaus, J. P.: Deglacial temperature history of West Antarctica, *Proc National Acad Sci*, 113, 14249–
815 14254, <https://doi.org/10.1073/pnas.1609132113>, 2016.

816 Curry, B. and Petras, J.: Chronological framework for the deglaciation of the Lake Michigan lobe of the Laurentide
817 Ice Sheet from ice-walled lake deposits, *J. Quaternary Sci.*, 26, 402–410, <https://doi.org/10.1002/jqs.1466>,
818 2011.

819 Dalton, A. S., Margold, M., Stokes, C. R., Tarasov, L., Dyke, A. S., Adams, R. S., Allard, S., Arends, H. E., Atkinson,
820 N., Attig, J. W., Barnett, P. J., Barnett, R. L., Batterson, M., Bernatchez, P., Borns, H. W., Breckenridge, A.,
821 Briner, J. P., Brouard, E., Campbell, J. E., Carlson, A. E., Clague, J. J., Curry, B. B., Daigneault, R.-A., Dubé-
822 Loubert, H., Easterbrook, D. J., Franzi, D. A., Friedrich, H. G., Funder, S., Gauthier, M. S., Gowan, A. S.,
823 Harris, K. L., Hétu, B., Hooyer, T. S., Jennings, C. E., Johnson, M. D., Kehew, A. E., Kelley, S. E., Kerr, D.,
824 King, E. L., Kjeldsen, K. K., Knaeble, A. R., Lajeunesse, P., Lakeman, T. R., Lamothe, M., Larson, P.,
825 Lavoie, M., Loope, H. M., Lowell, T. V., Lusardi, B. A., Manz, L., McMartin, I., Nixon, F. C., Occhietti, S.,
826 Parkhill, M. A., Piper, D. J. W., Pronk, A. G., Richard, P. J. H., Ridge, J. C., Ross, M., Roy, M., Seaman, A.,
827 Shaw, J., Stea, R. R., Teller, J. T., Thompson, W. B., Thorleifson, L. H., Utting, D. J., Veillette, J. J., Ward,
828 B. C., Weddle, T. K., and Wright, H. E.: An updated radiocarbon-based ice margin chronology for the last
829 deglaciation of the North American Ice Sheet Complex, *Quaternary Sci Rev*, 234, 106223,
830 <https://doi.org/10.1016/j.quascirev.2020.106223>, 2020.

831 Davis, M. B., Spear, R. W., and Shane, L. C. K.: Holocene climate of New England, *Quat. Res.*, 14, 240–250,
832 [https://doi.org/10.1016/0033-5894\(80\)90051-4](https://doi.org/10.1016/0033-5894(80)90051-4), 1980.

833 Davis, P. T., Bierman, P. R., Corbett, L. B., and Finkel, R. C.: Cosmogenic exposure age evidence for rapid Laurentide
834 deglaciation of the Katahdin area, west-central Maine, USA, 16 to 15 ka, *Quaternary Sci Rev*, 116, 95–105,
835 <https://doi.org/10.1016/j.quascirev.2015.03.021>, 2015.

836 Deevey: Radiocarbon-dated pollen sequences in eastern North America, *Veroffentlichungen des Geobotanischen*
837 *Institutes Rubel in Zurich*, 30, 1958.

838 Denton, G. H. and Hughes, T. J.: *The Last Great Ice Sheets*, Wiley-Interscience, New York, 464 pp., 1981.

839 Denton, G. H., Anderson, R. F., Toggweiler, J. R., Edwards, R. L., Schaefer, J. M., and Putnam, A. E.: The Last
840 Glacial Termination, *Science*, 328, 1652–1656, <https://doi.org/10.1126/science.1184119>, 2010.

841 Dorion, C. C., Balco, G. A., Kaplan, M. R., Kreutz, K. J., Wright, D., and Jr., H. W. B.: Stratigraphy,
842 paleoceanography, chronology, and environment during deglaciation of eastern Maine, in: *Special papers*
843 *(Geological Society of America)*, vol. 351, edited by: Weddle, T. K. and Retelle, M. J., 215,
844 <https://doi.org/10.1130/0-8137-2351-5.215>, 2001.

845 Drebber, J. S., Halsted, C. T., Corbett, L. B., Bierman, P. R., and Caffee, M. W.: In Situ Cosmogenic ^{10}Be Dating of
846 Laurentide Ice Sheet Retreat from Central New England, USA, *Geosciences*, 13, 213,

847 <https://doi.org/10.3390/geosciences13070213>, 2023.

848 Dyke, A. S.: An outline of North American deglaciation with emphasis on central and northern Canada, *Dev Quat Sci*,
849 2, 373–424, [https://doi.org/10.1016/s1571-0866\(04\)80209-4](https://doi.org/10.1016/s1571-0866(04)80209-4), 2004.

850 Frankel, L., and Thomas, H. F.: Evidence of freshwater lake deposits in Block Island Sound: *The Journal of Geology*,
851 v. 74, no. 2, p. 240-242, 1966.

852 Fuller, M. L.: *The Geology of Long Island New York*, US Geological Survey, 1914.

853 Glover, K. C., Lowell, T. V., Wiles, G. C., Pair, D., Applegate, P., and Hajdas, I.: Deglaciation, basin formation and
854 post-glacial climate change from a regional network of sediment core sites in Ohio and eastern Indiana, *Quat.*
855 *Res.*, 76, 401–410, <https://doi.org/10.1016/j.yqres.2011.06.004>, 2011.

856 Gregoire, L. J., Valdes, P. J., and Payne, A. J.: The relative contribution of orbital forcing and greenhouse gases to the
857 North American deglaciation, *Geophys Res Lett*, 42, 9970–9979, <https://doi.org/10.1002/2015gl066005>,
858 2015.

859 Hall, B. L., Borns, H. W., Bromley, G. R. M., and Lowell, T. V.: Age of the Pineo Ridge System: Implications for
860 behavior of the Laurentide Ice Sheet in eastern Maine, U.S.A., during the last deglaciation, *Quaternary Sci*
861 *Rev*, 169, 344–356, <https://doi.org/10.1016/j.quascirev.2017.06.011>, 2017.

862 Halsted, C. T., Bierman, P. R., Shakun, J. D., Davis, P. T., Corbett, L. B., Drebbler, J. S., and Ridge, J. C.: A critical
863 re-analysis of constraints on the timing and rate of Laurentide Ice Sheet recession in the northeastern United
864 States, *J. Quat. Sci.*, <https://doi.org/10.1002/jqs.3563>, 2023.

865 Halsted, C. T., Bierman, P. R., Shakun, J. D., Davis, P. T., Corbett, L. B., Caffee, M. W., Hodgdon, T. S., and Licciardi,
866 J. M.: Rapid southeastern Laurentide Ice Sheet thinning during the last deglaciation revealed by elevation
867 profiles of in situ cosmogenic ^{10}Be , *Gsa Bulletin*, <https://doi.org/10.1130/b36463.1>, 2022.

868 Harbor, J., Stroeven, A. P., Fabel, D., Clarhäll, A., Kleman, J., Li, Y., Elmore, D., and Fink, D.: Cosmogenic nuclide
869 evidence for minimal erosion across two subglacial sliding boundaries of the late glacial Fennoscandian ice
870 sheet, *Geomorphology*, 75, 90–99, <https://doi.org/10.1016/j.geomorph.2004.09.036>, 2006.

871 Hays, J. D., Imbrie, J., and Shackleton, N. J.: Variations in the Earth’s Orbit: Pacemaker of the Ice Ages, *Science*,
872 194, 1121–1132, <https://doi.org/10.1126/science.194.4270.1121>, 1976.

873 Heath, S. L., Loope, H. M., Curry, B. B., and Lowell, T. V.: Pattern of southern Laurentide Ice Sheet margin position
874 changes during Heinrich Stadials 2 and 1, *Quaternary Sci Rev*, 201, 362–379,
875 <https://doi.org/10.1016/j.quascirev.2018.10.019>, 2018.

876 Hooke, R. L., and H. B. Clausen: Wisconsin and holocene $\delta^{18}\text{O}$ variations, Barnes Ice Cap, Canada, *Geol. Soc. Am.*
877 *Bull.*, 93(8), 784–789, 1982.

878 Hooke, R. L.: Pleistocene ice and the base of the Barnes Ice Cap, Canada, *J. Glaciol.*, 17(75), 49–60, 1976.

879 Imbrie, J., Berger, A., Boyle, E. A., Clemens, S. C., Duffy, A., Howard, W. R., Kukla, G., Kutzbach, J., Martinson,
880 D. G., McIntyre, A., Mix, A. C., Molfino, B., Morley, J. J., Peterson, L. C., Pisias, N. G., Prell, W. L., Raymo,
881 M. E., Shackleton, N. J., and Toggweiler, J. R.: On the structure and origin of major glaciation cycles 2. The
882 100,000-year cycle, *Paleoceanography*, 8, 699–735, <https://doi.org/10.1029/93pa02751>, 1993.

883 Jaret, S. J., Tailby, N. D., Hammond, K. G., Rasbury, E. T., Wooton, K., Ebel, D. S., DiPadova, E., Smith, R., Yuan,
884 V., Jaffe, N., Smith, L. M., and Spaeth, L.: *Geology of Central Park, Manhattan, New York City, USA: New*
885 *geochemical insights*, *The Geological Society of America Field Guide* 61, 1–14,
886 [https://doi.org/10.1130/2020.0061\(02\)](https://doi.org/10.1130/2020.0061(02)), 2021.

887 Kaplan, M. R., Strelin, J. A., Schaefer, J. M., Denton, G. H., Finkel, R. C., Schwartz, R., Putnam, A. E., Vandergoes,
888 M. J., Goehring, B. M., and Travis, S. G.: In-situ cosmogenic ^{10}Be production rate at Lago Argentino,
889 Patagonia: Implications for late-glacial climate chronology, *Earth Planet Sc Lett*, 309, 21–32,
890 <https://doi.org/10.1016/j.epsl.2011.06.018>, 2011.

891 Kaplan, M. R.: Retreat of a tidewater margin of the Laurentide ice sheet in eastern coastal Maine between ca. 14 000
892 and 13 000 ^{14}C yr B.P., *GSA Bull.*, 111, 620–632, [https://doi.org/10.1130/0016-7606\(1999\)111<0620:roatmo>2.3.co;2](https://doi.org/10.1130/0016-7606(1999)111<0620:roatmo>2.3.co;2), 1999.

893
894 Kaye, C. A.: Early Postglacial Beavers in Southeastern New England, *Science*, 138, 906–907,

895 <https://doi.org/10.1126/science.138.3543.906>, 1962.

896 Kaye, C. A.: Geology of the Kingston Quadrangle, Rhode Island, Geological Survey Bulletin 1071-1, 15, 193–194,
897 1960.

898 Kaye, C. A.: Illinoian and early Wisconsinan moraines of Martha’s Vineyard, Massachusetts, US Geological Survey
899 Professional Paper 501-C., C140–C143, 1964a.

900 Kaye, C. A.: Outline of Pleistocene geology of Martha’s Vineyard, Massachusetts, US Geological Survey Professional
901 Paper 501-C, C134–C139, 1964b.

902 Kaye, C. A.: Preliminary surficial map of Martha’s Vineyard, Nomans Land, and parts of Naushon and Pasque Islands,
903 Massachusetts, US Geological Survey Open-File Report 72-205, 1972.

904 Kelly, M. A.: The Late Würmian Age in the Western Swiss Alps: Last Glacial Maximum (LGM) Ice-surface
905 Reconstruction and ¹⁰Be Dating of Late-glacial Features, 2003.

906 Kindler, P., Guillevic, M., Baumgartner, M., Schwander, J., Landais, A., and Leuenberger, M.: Temperature
907 reconstruction from 10 to 120 kyr b2k from the NGRIP ice core, *Clim Past*, 10, 887–902,
908 <https://doi.org/10.5194/cp-10-887-2014>, 2014.

909 Koteff, C. and Jr., F. P.: Systematic Ice Retreat in New England, in: Geological Survey Professional Paper 1179,
910 United States Government Printing Office, Washington, 1981.

911 Lal, D.: Cosmic ray labeling of erosion surfaces: in situ nuclide production rates and erosion models, *Earth Planet Sc
912 Lett*, 104, 424–439, [https://doi.org/10.1016/0012-821x\(91\)90220-c](https://doi.org/10.1016/0012-821x(91)90220-c), 1991.

913 Lambeck, K., Rouby, H., Purcell, A., Sun, Y., and Sambridge, M.: Sea level and global ice volumes from the Last
914 Glacial Maximum to the Holocene, *Proc National Acad Sci*, 111, 15296–15303,
915 <https://doi.org/10.1073/pnas.1411762111>, 2014.

916 Laskar, J., Robutel, P., Joutel, F., Gastineau, M., Correia, A. C. M., and Levrard, B.: A long-term numerical solution
917 for the insolation quantities of the Earth, *Astron Astrophys*, 428, 261–285, [https://doi.org/10.1051/0004-
918 6361:20041335](https://doi.org/10.1051/0004-6361:20041335), 2004.

919 Lifton, N., Sato, T., and Dunai, T. J.: Scaling in situ cosmogenic nuclide production rates using analytical
920 approximations to atmospheric cosmic-ray fluxes, *Earth Planet Sc Lett*, 386, 149–160,
921 <https://doi.org/10.1016/j.epsl.2013.10.052>, 2014.

922 Löfverström, M., Caballero, R., Nilsson, J., and Kleman, J.: Evolution of the large-scale atmospheric circulation in
923 response to changing ice sheets over the last glacial cycle, *Clim Past*, 10, 1453–1471,
924 <https://doi.org/10.5194/cp-10-1453-2014>, 2014.

925 Marcott, S. A., Bauska, T. K., Buizert, C., Steig, E. J., Rosen, J. L., Cuffey, K. M., Fudge, T. J., Severinghaus, J. P.,
926 Ahn, J., Kalk, M. L., McConnell, J. R., Sowers, T., Taylor, K. C., White, J. W. C., and Brook, E. J.:
927 Centennial-scale changes in the global carbon cycle during the last deglaciation, *Nature*, 514, 616–619,
928 <https://doi.org/10.1038/nature13799>, 2014.

929 McManus, J. F., Francois, R., Gherardi, J.-M., Keigwin, L. D., and Brown-Leger, S.: Collapse and rapid resumption
930 of Atlantic meridional circulation linked to deglacial climate changes, *Nature*, 428, 834–837,
931 <https://doi.org/10.1038/nature02494>, 2004.

932 McMaster, R. L.: Sediments of Narragansett Bay system and Rhode Island Sound, Rhode Island, *J Sediment Res*, 30,
933 249–274, <https://doi.org/10.1306/74d70a15-2b21-11d7-8648000102c1865d>, 1960.

934 McWeeney, L. J.: Revised vegetation history for the post-glacial period (15,200–10,000 14 C years B.P.) in southern
935 New England, in: Geological Society of America Abstracts with Programs 27, 1995.

936 Milankovitch, M.: Kanon der Erdbestrahlung und Seine Anwendung auf das Eiszeitenproblem, Special Publication.
937 Royal Serbian Academy, 33, 132, 1941.

938 Mills, H. C. and Wells, P. D.: Ice-Shove Deformation and Glacial Stratigraphy of Port Washington, Long Island, New
939 York, *Gsa Bulletin*, 85, 357–364, [https://doi.org/10.1130/0016-7606\(1974\)85<357:idadso>2.0.co;2](https://doi.org/10.1130/0016-7606(1974)85<357:idadso>2.0.co;2), 1974.

940 NASA Shuttle Radar Topography Mission (SRTM). Shuttle Radar Topography Mission (SRTM) Global.
941 Distributed by OpenTopography. <https://doi.org/10.5069/G9445JDF>. last access: 26 January 2024.

942 Needell, S. W., O'Hara, C. J., and Knebel, H. J.: Quaternary geology of the Rhode Island inner shelf: *Marine Geology*,
943 v. 53, p. 41-53, 1983.

944 Nishiizumi, K., Imamura, M., Caffee, M. W., Southon, J. R., Finkel, R. C., and McAninch, J.: Absolute calibration of
945 ^{10}Be AMS standards, *Nucl Instruments Methods Phys Res Sect B Beam Interactions Mater Atoms*, 258,
946 403–413, <https://doi.org/10.1016/j.nimb.2007.01.297>, 2007.

947 Nishiizumi, K.: ^{10}Be , ^{26}Al , ^{36}Cl , and ^{41}Ca AMS standards, in: 9th Conference on Accelerator Mass Spectrometry.
948 p. 130, 2002.

949 Oakley, B. A. and Boothroyd, J. C.: Constrained age of Glacial Lake Narragansett and the deglacial chronology of the
950 Laurentide Ice Sheet in southeastern New England, *J Paleolimnol*, 50, 305–317,
951 <https://doi.org/10.1007/s10933-013-9725-7>, 2013.

952 Oakley, B. A.: Late Quaternary Depositional Environments, Timing and Recent Deposition: Narragansett Bay, Rhode
953 Island and Massachusetts, Doctoral thesis, University of Rhode Island, 2012.

954 Oldale, R. N. and O'Hara, C. J.: Glaciotectonic origin of the Massachusetts coastal end moraines and a fluctuating
955 late Wisconsinan ice margin, *GSA Bulletin*, 95, 61–74, [https://doi.org/10.1130/0016-7606\(1984\)95<61:gootmc>2.0.co;2](https://doi.org/10.1130/0016-7606(1984)95<61:gootmc>2.0.co;2), 1984.

957 Oldale, R. N.: Pleistocene stratigraphy of Nantucket, Martha's Vineyard, the Elizabeth Islands, and Cape Cod,
958 Massachusetts, in: Late Wisconsinan Glaciation of New England: Proceedings of the Symposium, edited by:
959 Larson, G. J. and Stone, B. D., Kendall/Hunt, Dubuque, IA, 1–34, 1982.

960 Peteet, D. M., Beh, M., Orr, C., Kurdyla, D., Nichols, J., and Guilderson, T.: Delayed deglaciation or extreme Arctic
961 conditions 21-16 cal. kyr at southeastern Laurentide Ice Sheet margin?, *Geophys Res Lett*, 39, n/a-n/a,
962 <https://doi.org/10.1029/2012gl051884>, 2012.

963 Prince, K. K., Briner, J. P., Walcott, C. K., Chase, B. M., Kozlowski, A. L., Rittenour, T. M., and Yang, E. P.: New
964 age constraints reveal moraine stabilization thousands of years after deposition during the last deglaciation
965 of western New York, USA, *EGUsphere* [preprint], <https://doi.org/10.5194/egusphere-2023-2655>, 2024.

966 Putnam, A. E., Bromley, G. R. M., Rademaker, K., and Schaefer, J. M.: In situ ^{10}Be production-rate calibration from
967 a ^{14}C -dated late-glacial moraine belt in Rannoch Moor, central Scottish Highlands, *Quat Geochronol*, 50,
968 109–125, <https://doi.org/10.1016/j.quageo.2018.11.006>, 2019.

969 Raymo, M. E.: The timing of major climate terminations, *Paleoceanography*, 12, 577–585,
970 <https://doi.org/10.1029/97pa01169>, 1997.

971 Refsnider, K.A., Miller, G.H., Fogel, M.L., Fréchette, B., Bowden, R., Andrews, J.T., Farmer, G.L.: Subglacially
972 precipitated carbonates record geochemical interactions and pollen preservation at the base of the Laurentide
973 Ice Sheet on central Baffin Island, eastern Canadian Arctic. *Quaternary Res* 81, 94–105.
974 <https://doi.org/10.1016/j.yqres.2013.10.014>, 2014.

975 Reimer, G. E.: The Sedimentology and Stratigraphy of the Southern Basin of Glacial Lake Passaic, New Jersey,
976 Master's thesis, Rutgers University, New Brunswick, New Jersey, 1984.

977 Reimer, P. J., Austin, W. E. N., Bard, E., Bayliss, A., Blackwell, P. G., Ramsey, C. B., Butzin, M., Cheng, H., Edwards,
978 R. L., Friedrich, M., Grootes, P. M., Guilderson, T. P., Hajdas, I., Heaton, T. J., Hogg, A. G., Hughen, K. A.,
979 Kromer, B., Manning, S. W., Muscheler, R., Palmer, J. G., Pearson, C., Plicht, J. van der, Reimer, R. W.,
980 Richards, D. A., Scott, E. M., Southon, J. R., Turney, C. S. M., Wacker, L., Adolphi, F., Büntgen, U., Capano,
981 M., Fahrni, S. M., Fogtmann-Schulz, A., Friedrich, R., Köhler, P., Kudsk, S., Miyake, F., Olsen, J., Reinig,
982 F., Sakamoto, M., Sookdeo, A., and Talamo, S.: The IntCal20 Northern Hemisphere Radiocarbon Age
983 Calibration Curve (0–55 cal kBP), *Radiocarbon*, 62, 725–757, <https://doi.org/10.1017/rdc.2020.41>, 2020.

984 Ridge, J. C., Balco, G., Bayless, R. L., Beck, C. C., Carter, L. B., Dean, J. L., Voytek, E. B., and Wei, J. H.: The new
985 North American Varve Chronology: A precise record of southeastern Laurentide Ice Sheet deglaciation and
986 climate, 18.2-12.5 kyr BP, and correlations with Greenland ice core records, *Am J Sci*, 312, 685–722,
987 <https://doi.org/10.2475/07.2012.01>, 2012.

988 Ridge, J. C.: The Quaternary glaciation of western New England with correlations to surrounding areas, *Dev Quat*
989 *Sci*, 2, 169–199, [https://doi.org/10.1016/s1571-0866\(04\)80196-9](https://doi.org/10.1016/s1571-0866(04)80196-9), 2004.

990 Rittenour, T.M., Stone, B.D., and Mahan, S.: Application of OSL dating to glacial deposits in southern Massachusetts:
991 Refining the chronology and addressing questions related to solar resetting in glacial environments,
992 Geological Society of America Abstracts with Programs, 44 (2), p. 86, 2012.

993 Schaefer, J. M., Denton, G. H., Kaplan, M., Putnam, A., Finkel, R. C., Barrell, D. J. A., Andersen, B. G., Schwartz,
994 R., Mackintosh, A., Chinn, T., and Schlüchter, C.: High-Frequency Holocene Glacier Fluctuations in New
995 Zealand Differ from the Northern Signature, *Science*, 324, 622–625,
996 <https://doi.org/10.1126/science.1169312>, 2009.

997 Schafer, J. P. and Hartshorn, J. H.: The Quaternary of New England, in: *The Quaternary of the United States*, edited
998 by: Jr., H. E. W. and Frey, D. G., Princeton University Press, Princeton, NJ, 113–127, 1965.

999 Schafer, J. P.: Surficial Geologic Map of the Watch Hill quadrangle, Rhode Island-Connecticut, scale 1:24,000, 1965.

1000 Schuldenrein, J. and Aiuvalasit, M.: Urban geoarchaeology and sustainability: A case study from Manhattan Island,
1001 New York City, USA, in: *Geoarchaeology, Climate Change, and Sustainability: Geological Society of*
1002 *America Special Paper 476*, edited by: Brown, A. G., Basell, L. S., and Butzer, K. W.,
1003 [https://doi.org/10.1130/2011.2476\(12\)](https://doi.org/10.1130/2011.2476(12)), 2011.

1004 Shakun, J. D., Clark, P. U., He, F., Lifton, N. A., Liu, Z., and Otto-Bliesner, B. L.: Regional and global forcing of
1005 glacier retreat during the last deglaciation, *Nat Commun*, 6, 8059, <https://doi.org/10.1038/ncomms9059>,
1006 2015.

1007 Sinclair, S. N., Licciardi, J. M., Campbell, S. W., and Madore, B. M.: Character and origin of De Geer moraines in
1008 the Seacoast region of New Hampshire, USA: *Journal of Quaternary Science*, v. 33, no. 2, p. 225-237, 2018.

1009 Sirkin, L. and Stuckenrath, R.: The Portwashingtonian warm interval in the northern Atlantic coastal plain, *GSA*
1010 *Bulletin*, 91, 332–336, [https://doi.org/10.1130/0016-7606\(1980\)91<332:tpwiiit>2.0.co;2](https://doi.org/10.1130/0016-7606(1980)91<332:tpwiiit>2.0.co;2), 1980.

1011 Sirkin, L., 1986. Pleistocene stratigraphy of Long Island, New York, in: Cadwell, D.H. (Eds.), *The Wisconsinan Stage*
1012 *of the First Geological District, Eastern New York*. New York State Museum, Albany, NY.

1013 Sirkin, L.: Block Island, Rhode Island: Evidence of fluctuation of the late Pleistocene ice margin, *GSA Bulletin*, 87,
1014 574–580, [https://doi.org/10.1130/0016-7606\(1976\)87<574:birieo>2.0.co;2](https://doi.org/10.1130/0016-7606(1976)87<574:birieo>2.0.co;2), 1976.

1015 Sirkin: Late Wisconsinan glaciation of Long Island, New York, to Block Island, Rhode Island, 35–59, 1982.

1016 Soren, J.: Geologic and geohydrologic reconnaissance of Staten Island, New York, U.S Geological Survey, Water-
1017 Resources Investigations Report 87-4048, <https://doi.org/10.3133/wri874048>, 1988.

1018 Stanford, S. D. and Harper, D.: Glacial lakes of the lower Passaic, 13, 271–286, 1991.

1019 Stanford, S. D., Stone, B. D., Ridge, J. C., Witte, R. W., Pardi, R. R., and Reimer, G. E.: Chronology of Laurentide
1020 glaciation in New Jersey and the New York City area, United States, *Quaternary Res*, 99, 142–167,
1021 <https://doi.org/10.1017/qua.2020.71>, 2021.

1022 Stanford, S. D.: Late Wisconsinan glacial geology of the New Jersey Highlands, *Northeastern Geology*, 210–223,
1023 1993.

1024 Stanford, S. D.: Onshore record of Hudson River drainage to the continental shelf from the late Miocene through the
1025 late Wisconsinan deglaciation, U.S.A.: synthesis and revision, *Boreas*, 1–17, 2010.

1026 Stokes, C. R., Tarasov, L., and Dyke, A. S.: Dynamics of the North American Ice Sheet Complex during its inception
1027 and build-up to the Last Glacial Maximum, *Quaternary Sci Rev*, 50, 86–104,
1028 <https://doi.org/10.1016/j.quascirev.2012.07.009>, 2012.

1029 Stokes, C. R.: Deglaciation of the Laurentide Ice Sheet from the Last Glacial Maximum, *Cuadernos De Investigación*
1030 *Geográfica*, 43, 377–428, <https://doi.org/10.18172/cig.3237>, 2017.

1031 Stone, B. D. and Borns, H. W. Jr.: Pleistocene glacial and interglacial stratigraphy of New England, Long Island, and
1032 adjacent Georges Bank and Gulf of Maine, *Quaternary Sci Rev*, 5, 39–52, [https://doi.org/10.1016/0277-](https://doi.org/10.1016/0277-3791(86)90172-1)
1033 [3791\(86\)90172-1](https://doi.org/10.1016/0277-3791(86)90172-1), 1986.

1034 Stone, B. D., Stanford, S. D., and Witte, R. W.: Surficial Geologic Map of Northern New Jersey, Miscellaneous
1035 Investigations Series Map I-2540-C, U.S. Geological Survey, Reston, VA, 2002.

1036 Stone, B. D., Stanford, S. D., and Witte, R. W.: Surficial Geologic Map of the Northern Sheet, New Jersey, US
1037 Geological Survey, U.S. Geological Survey Open File Map OF 95-543B, 1995.

- 1038 Stone, B.D., and Stone, J.R.: Geologic Origins of Cape Cod, Massachusetts; Guidebook for the Northeast Friends of
1039 the Pleistocene, 82 nd Annual Fieldtrip, May 31-June 2, 2019: Massachusetts Geological Survey Open-file
1040 Report 19-01, 63 p, <https://www2.newpaltz.edu/fop/pdf/FOP2019Guide.pdf>, 2019.
- 1041 Stone, J. R., Stone, B. D., DiGiacomo-Cohen, M. L., and Mabee, S. B.: Surficial Materials of Massachusetts— A
1042 1:24,000-Scale Geologic Map Database, USGS Scientific Investigations Map 3402,
1043 <https://doi.org/10.3133/sim3402>, 2018.
- 1044 Stone, J. O., Balco, G. A., Sugden, D. E., Caffee, M. W., III, L. C. S., Cowdery, S. G., and Siddoway, C.: Holocene
1045 Deglaciation of Marie Byrd Land, West Antarctica, *Science*, 299, 99–102,
1046 <https://doi.org/10.1126/science.1077998>, 2003.
- 1047 Stone, J. O.: Air pressure and cosmogenic isotope production, *J Geophys Res Solid Earth*, 105, 23753–23759,
1048 <https://doi.org/10.1029/2000jb900181>, 2000.
- 1049 Stone, J. R., Schafer, J. P., London, E. H., DiGiacomo-Cohen, M. L., Lewis, R. S., and Thompson, W. B.: Quaternary
1050 Geologic Map of Connecticut and Long Island Sound Basin, U.S. Geological Survey, 2005.
1051 <https://doi.org/10.3133/sim2784>
- 1052 Stone, J. R., Shafer, J. P., London, E. H., DiGiacomo-Cohen, M., Lewis, R. S., and Thompson, W. B.: Quaternary
1053 Geologic Map of Connecticut and Long Island Sound Basin: : U.S. Geological Survey Geologic
1054 Investigations Series Map I-2784, scale 1:125,000, 2 sheets and pamphlet. p. 1-72, 2005.
- 1055 Stone, J. R.: Surficial Materials Map of the Chipuxet River and Chickasheen Brook Basins, Rhode Island, U.S.
1056 Geological Survey, 2014.
- 1057 Taterka, B. D.: Bedrock geology of Central Park, New York City, M.S. Thesis University of Massachusetts Depart-
1058 ment of Geology and Geography, Contribution 61, 1987.
- 1059 Todd, B. J., Valentine, P. C., Longva, O., and Shaw, J.: Glacial landforms on German Bank, Scotian Shelf: evidence
1060 for Late Wisconsinan ice-sheet dynamics and implications for the formation of De Geer moraines: *Boreas*,
1061 v. 36, no. 2, p. 148-169, 2007.
- 1062 Tucholke and Hollister, B. E.: Late Wisconsin glaciation of the southwestern Gulf of Maine: new evidence from the
1063 marine environment, *GSA Bulletin* 84, 279–3296, 1973.
- 1064 Tzedakis, P. C., Drysdale, R. N., Margari, V., Skinner, L. C., Menviel, L., Rhodes, R. H., Taschetto, A. S., Hodell, D.
1065 A., Crowhurst, S. J., Hellstrom, J. C., Fallick, A. E., Grimalt, J. O., McManus, J. F., Martrat, B., Mokeddem,
1066 Z., Parrenin, F., Regattieri, E., Roe, K., and Zanchetta, G.: Enhanced climate instability in the North Atlantic
1067 and southern Europe during the Last Interglacial, *Nat Commun*, 9, 4235, [https://doi.org/10.1038/s41467-018-](https://doi.org/10.1038/s41467-018-06683-3)
1068 [06683-3](https://doi.org/10.1038/s41467-018-06683-3), 2018.
- 1069 Ullman, D. J., Carlson, A. E., LeGrande, A. N., Anslow, F. S., Moore, A. K., Caffee, M., Syverson, K. M., and
1070 Licciardi, J. M.: Southern Laurentide ice-sheet retreat synchronous with rising boreal summer insolation,
1071 *Geology*, 43, 23–26, <https://doi.org/10.1130/g36179.1>, 2015.
- 1072 Ullman, D. J., LeGrande, A. N., Carlson, A. E., Anslow, F. S., and Licciardi, J. M.: Assessing the impact of Laurentide
1073 Ice Sheet topography on glacial climate, *Clim Past*, 10, 487–507, <https://doi.org/10.5194/cp-10-487-2014>,
1074 2014.
- 1075 Upham, W.: Terminal moraines of the North American ice sheet, *American Journal of Science*, s3-18, 197,
1076 <https://doi.org/10.2475/ajs.s3-18.105.197>, 1879.
- 1077 Woodworth, J. B. and Wigglesworth, E.: Geography and geology of the region including Cape Cod, the Elizabeth
1078 islands, Nantucket, Marthas Vineyard, No Mans Land and Block Island, by J. B. Woodworth and Edward
1079 Wigglesworth, Printed for the Museum, Cambridge, Mass, 1934.
- 1080 Wroblewski, E. A., and Hooke, R. L.: Deglaciation of Penobscot Bay, Maine, USA: *Atlantic Geology*, v. 56, p. 147-
1081 161, 2020.
- 1082 Young, N. E., Briner, J. P., Maurer, J., and Schaefer, J. M.: ^{10}Be measurements in bedrock constrain erosion beneath
1083 the Greenland Ice Sheet margin, *Geophys Res Lett*, 43, 11,708-11,719,
1084 <https://doi.org/10.1002/2016gl070258>, 2016.
- 1085 Young, N. E., Schaefer, J. M., Briner, J. P., and Goehring, B. M.: A ^{10}Be production-rate calibration for the Arctic, *J*

1086 Quaternary Sci, 28, 515–526, <https://doi.org/10.1002/jqs.2642>, 2013.
1087
1088
1089
1090